Wheat Genetic Loci Conferring Resistance to Yellow Rust in the Face of Recent Epidemics of Genetically Diverse Races of the Fungus Puccinia Striiformis F. Sp. Tritici

Laura Bouvet
NIAB: National Institute of Agricultural Botany
Lawrence Percival-Alwyn
NIAB: National Institute of Agricultural Botany
Simon Berry
Limagrain UK Ltd.
Paul Fenwick
Limagrain UK Ltd.
Camila Campos Mantello
NIAB: National Institute of Agricultural Botany
Sarah Holdgate
NIAB: National Institute of Agricultural Botany
Ian Mackay
NIAB: National Institute of Agricultural Botany
James Cockram (James.Cockram@niab.com)
NIAB https://orcid.org/0000-0002-1014-6463

Research Article

Keywords: Bread wheat (Triticum aestivum L.), yellow rust, stripe rust, quantitative trait loci (QTL), multi-parent advanced generation inter-cross (MAGIC), marker-assisted selection (MAS)

Posted Date: April 27th, 2021

DOI: https://doi.org/10.21203/rs.3.rs-459064/v1

Wheat genetic loci conferring resistance to yellow rust in the face of recent epidemics of genetically diverse races of the fungus *Puccinia striiformis* f. sp. *tritici*

Laura Bouvet[1,2], Lawrence Percival-Alwyn[1], Simon Berry[3], Paul Fenwick[3], Camila Campos Mantello[1], Sarah Holdgate[1], Ian J. Mackay[1†], James Cockram[1*]

[1]NIAB, 93 Lawrence Weaver Road, Cambridge, CB3 0LE, United Kingdom

[2]Department of Plant Sciences, University of Cambridge, Downing Street, Cambridge, CB2 3EA, United Kingdom

[3]Limagrain UK Ltd, Market Rasen, LN7 6DT, United Kingdom

[†]Current address: SRUC, The King's Buildings, West Mains Road, Edinburgh, EH9 3JG, United Kingdom

[*]Corresponding author: james.cockram@niab.com. ORCID: http://orcid.org/0000-0002-1014-6463

Key words: Bread wheat (*Triticum aestivum* L.), yellow rust, stripe rust, quantitative trait loci (QTL), multi-parent advanced generation inter-cross (MAGIC), marker-assisted selection (MAS)

Abstract

Yellow rust (YR), or stripe rust, is a major fungal disease of wheat (*Triticum aestivum*) caused by *Puccinia striiformis* f. sp. *tritici* (*Pst*). Since 2011, the historically clonal European *Pst* races have been superseded by the rapid incursion of genetically diverse lineages, reducing the resistance of varieties that previously showed durable resistance. Identification of sources of genetic resistance to such races is a high priority for wheat breeding. Here we use a wheat eight-founder multi-parent population genotyped with a 90,000 feature single nucleotide polymorphism array to genetically map adult plant YR resistance to such new *Pst* races. Analysis of five trials, at three sites in the UK, consistently identified four highly significant quantitative trait loci (QTL) across all test environments, located on chromosomes 1A (*QYr.niab-1A.1*), 2A (*QYr.niab-2A.1*), 2B (*QYr.niab-2B.1*) and 2D (*QYr.niab-2D.1*). Together these explained ~50% of the phenotypic variation, and genetic markers were developed that distinguished resistant and susceptible alleles. Analysis of these QTL in two-way and three-way combinations showed combinations conferred greater resistance than single QTL. Four additional major-effect QTL were detected in two or more trials, together explaining 15-20% of the phenotypic variation, as well as six minor QTL. Genomic analysis found the median physical interval size of these eight QTL to be 19.8 Mbp, and *QYr.niab-2A.1* and *QYr.niab-2D.1* to be at homoeologous locations on the group-2 chromosomes. Notably, the *QYr.niab-2B.1* physical interval contained five nucleotide-binding leucine-rich repeat (NLR) candidate genes with integrated BED domains, of which two corresponded to the cloned resistance genes *Yr7* and *Yr5/YrSp*.

Key message

Genetic analysis of a wheat multi-founder population identified 14 yellow rust resistance QTL. For the four most significant QTL, additive effects were demonstrated, and genetic markers validated for marker-assisted selection.

Introduction

Yellow rust (YR), caused by the biotrophic fungus *Puccinia striiformis* f. sp. *tritici* (*Pst*), is a widespread pathogen of wheat (*Triticum aestivum* L.), and a substantial threat to global wheat production. Since the 2000s, a subset of genetically diverse and divergent *Pst* lineages have been responsible for recurrent YR epidemics in numerous wheat-producing regions (Ali et al. 2014; 2017). The rapid adaptation and subsequent spread of these lineages into previously hostile environments has given rise to more aggressive pathotypes that are generally better adapted to higher temperatures (Milus et al. 2009). In the United Kingdom (UK) and North-Western Europe, the historically clonal *Pst* population has been largely displaced by a genetically diverse group of lineages (Hubbard et al. 2015; Hovmoller et al. 2016). First detected simultaneously in 2011 across several European countries, the 'Warrior' and 'Kranich' *Pst* races likely originated in the near Himalayan region and rapidly spread throughout the continent as a group of genetically distinct lineages. The ability of *Pst* to migrate over long distances, to locally adapt to new environments, and for new lineages to rapidly displace established populations, has had a notable impact on the resistant levels of wheat varieties in the UK (Hubbard et al. 2015; Bueno-Sancho et al. 2017) and beyond (Wellings, 2011; Hovmøller et al. 2016), prompting a review of YR resistance breeding and deployment strategies.

The most efficient way to control the effects of wheat fungal disease is via approaches that combine agricultural and agronomic practices, disease monitoring and genetic improvement of the wheat varieties grown (Downie et al. 2020). Resistance breeding focuses on two classes of rust resistance (*R*) genes. The first, termed 'seedling resistance' or 'all stage resistance', confers qualitative resistance, typically to one or a few *Pst* isolates. The second, termed 'adult plant resistance', typically provides quantitative resistance against multiple pathogen races. Over 300 genomic regions conferring YR resistance in wheat have been reported (Rosewarne et al. 2013; Wang & Chen, 2017). Of these, approximately 80 are permanently named yellow rust resistance (*Yr*) genes, recently summarised by Jamil et al. (2020). To date, 16 *R* genes controlling seedling resistance to different wheat rust pathogens have been cloned, and all encode nucleotide-binding leucine-rich repeat (NLR) proteins: *Lr1* (Cloutier et al. 2007), *Lr10* (Feuillet el al. 2003), *Lr21* (Huang et al. 2003), *Lr22a* (Thind et al. 2017), *Rga2* (Loutre et al. 2009), *Sr13* (Zhang et al. 2017), *Sr22* (Steuernagel et al., 2016), *Sr33* (Periyannan et al. 2013), *Sr35* (Saintenac et al. 2013), *Sr45* (Steuernagel et al. 2016), *Sr46* and *SrTA1662* (Arora et al.

2019), *Sr50* (Mago et al. 2015), *Yr7* and *Yr5/YrSP* (Marchal et al. 2018). Similarly, wheat *R* genes to other fungal pathogens are also encoded by *NLR* genes, such as the powdery mildew resistance genes *Pm2* (Sánchez-Martin et al. 2016), *Pm3b* (Yahiaoui et al. 2004), *Pm8* (Hurni et al. 2013), *Pm21* (He et al. 2018) and *Pm41* (Li et al. 2020). Host NLR proteins predominantly act by recognising the effector molecules that pathogens produce to inhibit host defence responses (Jones et al. 2016). To detect the large range of potential infecting pathogens, plant NLR gene families have radiated and diversified, commonly by localised gene duplication, unequal crossing-over, and variation within the leucine-rich repeat (LRR) domains which bind pathogen effectors (Sarris et al. 2016). Some NLRs have evolved to include a variety of additional 'integrated' domains that may be involved in receptor activation or downstream signalling (Sarris et al. 2016), most commonly kinase and DNA-binding domains (Anderson et al. 2020; Steuernagel et al. 2020). Examples include the BED zinc finger domain in *Yr7* and two alleles at a closely located paralogous gene termed *Yr5* and *YrSp* (Marchal et al. 2018), as well as the serine/threonine protein kinase (S/TPK) domain encoded by the wheat gene *Tsn1* conferring sensitivity to the necrotrophic fungal pathogens that cause tan spot and Septoria nodorum blotch (Faris et al. 2010). NLRs can also act by monitoring the status of host receptor proteins, termed 'indirect recognition'. For example, the Arabidopsis NLRs RPM1 and RPS2 monitor RPM1-interacting protein 4 (RIN4) for cleavage or phosphorylation by several bacterial effectors (Mackey et al. 2002; Axtell et al. 2003; Andersson et al. 2006). RIN4 acts as a susceptibility factor, but is also essential for normal plant growth (Mackey et al. 2002). Recently a wheat YR susceptibility gene encoding a branched-chain amino acid aminotransferase, *TaBCAT1*, has been identified via analysis of genes upregulated after *Pst* infection (Corredor-Moreno et al. 2021), although its mutation as single and double mutants in tetraploid wheat was not reported as affecting non-disease phenotypes. In contrast to seedling resistance genes, each of the three map-based cloned YR adult plant resistance genes encode a different class of protein: *Yr18/Lr34* an ABC transporter (Krattinger et al. 2009), *Yr36* a kinase-START domain protein (Fu et al. 2009), *Yr46/Lr67* a hexose transporter (Moore et al. 2015) and *Yr15/YrG303/YrH52* a kinase-pseudokinase protein (Klymiuk et al. 2018; 2020). Wheat breeding strategies historically focused on the use of qualitative yellow rust resistance genes, sometimes in isolation. *Yr17* for example was a popular source of such resistance in North-Western Europe. The effectiveness of the genetic resistance conferred by *Yr17* stopped soon after its deployment as a single resistance gene over a large wheat acreage (Bayles et al. 2000), although more recently this locus, or one genetically linked to it, provides resistance against Warrior *Pst* isolates. Where possible, resistance breeding strategies now favour the more

durable approach of combining race specific and non-race specific resistance genes to provide broad-spectrum resistance (Singh et al. 2005; Chen et al. 2013). Such use of genetic resistance will continue to be aided by the genetic and molecular characterisation of *Yr* genes and quantitative trait loci (QTL), understanding of how these genetic loci interact with each other, and molecular markers to track favourable alleles and allelic combinations in breeding programmes.

YR resistance QTL and *Yr* genes have predominantly been identified in biparental (e.g. Rosewarne et al. 2013) and association mapping panels (e.g. Maccaferri et al. 2015; Zegeye et al. 2014; Kertho et al. 2015). The crossing of just two parents in a biparental population inevitably limits the number of resistance genes and alleles that can be investigated (Mackay, 2001). While association mapping panels overcome this limitation by exploiting historical recombination events in the germplasm collection used, population structure in such collections can lead to false marker-trait associations (Cockram & Mackay 2018). Multi-founder populations (reviewed by Cockram & Mackay, 2018; Scott et al. 2020) now provide complementary resources for the genetic investigation of wheat disease resistance. Such designs include multiparent advanced generation inter cross (MAGIC) populations, derived by inter-crossing all founders over multiple generations before the generation of inbred lines. As each MAGIC progeny line likely contains alleles from all founders dispersed throughout its genetic background, MAGIC populations allow the effects of multiple alleles to be assessed within a single unified population. We previously developed the eight-founder 'NIAB Elite MAGIC' population, estimated to capture >80% of the genetic variation observed in UK wheat based on single nucleotide polymorphism (SNP) analysis (Mackay et al. 2014). Here we analyse this MAGIC population for resistance to YR at five trials conducted over two seasons and three sites in the United Kingdom (UK). Eight major adult plant resistance QTL were resolved, identified across growth seasons in which the new genetically diverse 'Warrior' group of *Pst* races were endemic in the UK. The gene space of these genetic loci was explored, candidate genes identified, and genetic markers tagging resistant haplotypes validated for the four most significant QTL. Additionally, six minor effect QTL were identified. Collectively, this work highlights the role of combinations of adult plant YR resistance genes in the genetic control of the aggressive *Pst* pathotypes that have replaced the previous asexual populations of the pathogen.

Methods

Germplasm, trial design, and field trials

The 'NIAB Elite MAGIC' wheat population (Mackay et al. 2014) consists of eight founders (the winter varieties Alchemy, Brompton, Claire, Hereward, Rialto, Robigus, Soissons, and the facultative variety Xi19) inter-crossed over three generations, and the outputs of the crossing then selfed over multiple generations to produce >1,000 recombinant inbred lines (RILs). The population was grown in five field trials over two seasons (YR assessment seasons 2015 and 2016) at three sites in the UK: (1) NIAB-Cambridge trial ground (latitude 52.235010, longitude 0.097871), Osgodby (latitude 53.410161, longitude -0.386770) and Rothwell (latitude 53.482597, longitude -0.259779). All trials followed an incomplete randomised block design generated with the DEW experimental design software, formerly www.expdesigns.co.uk but superseded by the R package 'blocksdesign' (Edmundson, 2020). The numbers of MAGIC RILs and control lines assessed at each site and year combination is listed in Table 1 and Supplementary Table 1. Seed for each season's trials were sourced from nursery plots grown the preceding season. Accordingly, RIL_9 and RIL_{10} seed were used for the 2015 and 2016 season trials, respectively. Standard agronomy practices were used for commercial wheat production at each location, but lacking application of chemical protection against YR. All trials were Autumn sown in the calendar year preceding YR assessment. Each line was sown in two 1-m rows, with six rows per plot. At the NIAB trial ground in Cambridgeshire, the central two rows were sown with the spreader wheat variety Vuka, known to be highly susceptible to all known UK races of YR, with RILs on either side. At the Osgodby and Rothwell sites in Lincolnshire, the central two rows were left empty. Instead, Vuka was present as a whole plot every three traverses. All trials apart from OSG16 were inoculated with a mixture of *Pst* races ('Solstice race' isolate 08/21 virulent on *Yr 1,2,3,4,6,9,17,25,32* and 'Warrior race' isolate 11/08 virulent on *Yr 1,2,3,4,6,79,17,25,32,Sp*). Trial OSG16 was un-inoculated, and therefore exposed only to natural YR infection.

Phenotypic data

YR infection severity of the leaves was assessed as the percentage of total leaf tissue with sporulating uredinia, estimated using the modified Cobb's scale (Peterson et al. 1948) ranging from 0 to 100 % infection (%inf). Leaf infection severity was assessed on three to four occasions at 12-18 day intervals at each trial, from the end of booting (Zadocks growth stage 45-49) until the mid-to-hard-dough stage (growth stage 85-87).

Trials analysis

A stepwise model selection approach was used to estimate the Best Linear Unbiased Estimators (BLUEs) for MAGIC RILs, integrating spatial and non-spatial mixed methods based on Restricted Maximum Likelihood (REML) implemented in Genstat, 18th edition (VSN International, 2015). Three models were considered: Model 1 – Blocking (genetic effects are estimated based only on the inter- and intra-block variation recovered from the model); Model 2 – Spatial (only considers global and/or local field trends); Model 3 - Spatial + blocking (combination of the above models). Initially, each model was optimised by including field trends running in either row or column direction or scoring order (the route used to score the trial), followed by between-model comparison to select the one that best fits the data. Further details of the three models used is given in Supplementary Text 1. The Akaike Information Criterion (AIC) was used as a measure for model selection (Akaike, 1974). Each model was optimised using AIC as a measure of model fit improvement, and the model with the lowest AIC value selected. Natural log transformation of the disease severity data was performed in cases where residuals were observed not to be normally distributed (trials NIAB16 and OSG16), to improve the normality of the residuals. These were assessed visually with histograms illustrating the distribution of the residuals and Q-Q normality plots. The Shapiro-Wilk normality test was used to further support these observations. Broad sense heritability (h^2) was used as a measure of total phenotypic variation attributable to the genotypic effect. The VHERITABILITY function in Genstat (18th edition, VSN International 2015) was used to calculate h^2 for each trial, and is based on the definition of heritability given by Cullis et al. (2006) and Piepho et al. (2007).

Genetic analysis

Genetic analysis was carried out using the 7,369 SNPs mapped to unique positions on the MAGIC genetic map (Gardner et al. 2016). For all trials, two broad methods were used for genetic analysis. (1) Single marker analysis (SMA): regression against allelic state at single markers using R/lme4 (Bates et al. 2015) in R (R Core Team, 2017) using the following mixed model:

$$Y = \mu_x + G_m + \beta + e$$

where Y is the YR resistance value, μ is the adjusted YR score for MAGIC RIL x, G_m is the fixed SNP marker effect, β is the population structure consisting of 'funnels' and 'plants within

funnels' effects (from Mackay et al. 2014), and e as the residual error term. The model has one degree of freedom, since regression is carried out on binary allelic state. Multiple-test correction was carried out using R/qvalue (Storey 2015), with a threshold of q<0.05. (2) Haplotype-based analysis, for which founder haplotype probabilities were calculated with the mpprob function in R/mpMap (Huang et al. 2011) with a threshold of 0.5. Three types of haplotype-based analyses were conducted. Identity by descent (IBD): regression against haplotype probability estimates using R/qtl and the following mixed model:

$$Y = \mu + G_p + \beta + e$$

where Y, μ, β and e are as for SMA above, and G_p is the fixed term for founder probabilities. Here, the statistical model has up to seven degrees of freedom. A QTL significance threshold q<0.05 was used. Interval mapping (IM): conducted in R/mpMap using the haplotype probability estimates. Composite interval mapping (CIM): conducted in R/mpMap with 10 covariates using the haplotype probability estimates. Within mpMap, an automated forward selection process based on AIC values was used to select the best ten marker covariates for each MAGIC line. Significant QTLs were then selected in two stages. First, mpMap scans the 100 markers surrounding a particular marker location and selects QTLs based on a threshold of –log10(p)>3. The number of significant QTL were then reduced by fitting a model with p<0.05 and with phenotypic variance explained (PVE)>0.5%. Significance threshold was estimated based on the simulation of the null distribution. Additionally, R/mpMap outputs founder contributions for each significant QTL, computed using a regression approach at each marker location. To summarise the results of the four analyses, the p or q values from each mapping method for all adjusted and log transformed YR scores, and for all environments, were compiled into a single table and a 'consensus' peak marker for each QTL identified following the methods described in Supplementary Text 2. 'Major' and 'minor' QTL were defined as those explaining either >5% or <5% of the phenotypic variance, respectively.

Bioinformatic analysis

The locations of the genetically mapped MAGIC SNPs on the physical map were determined using the SNP flanking DNA sequences (Wang et al. 2014) as queries for BLASTn (Altschul et al. 1990) interrogation of the wheat reference genome assembly (IWGSC, 2018). Where BLASTn hits of equal match were identified on more than one chromosome, genetic map position (Gardner et al. 2016) was used to assign BLASTn hits to chromosomes. For analysis of the YR QTL physical intervals in the context of disease resistance gene density, likely

resistant genes were first identified from the IWSGC RefSeq v1.0 assembly (IWSGC, 2018) high- and low-confidence gene functional annotations from v1.0 mapped on to gene model annotation RefSeq v1.1 (Alaux et al. 2018) where transcript.1 contained any of the following search terms: 'NB-LRR'; 'NBS-LRR'; 'NB-ARC'; 'TIR-NBS'; 'LRR family protein'; 'Leucine-rich repeat domain'; 'Plant disease resistance response'; 'Nucleotide binding site leucine-rich repeat'; 'disease resistance protein (TIR class)'. The percentile ranks of all gene counts and resistant gene counts for each QTL were calculated using windows of the same lengths (9.85 – 133.91 Mbp) sampling the genome (all 21 chromosomes plus the unassigned chromosome) every 100 bp. Plots were generated using the Circos visualization tool (Krzywinski et al. 2009). QTL resistant gene enrichment *p*-values were calculated using the binomial cumulative probability function where the chance of success is 0.365 (genome wide, resistant genes / total genes), the number of tests is the number of genes within the QTL and the number of successes is the number of resistant genes within the QTL.

Development of KASP markers

Selected SNPs from the 90k array were converted to the Kompetitive Allele-Specific PCR (KASP) genotyping system. SNP genomic flanking sequences were obtained from the T3 Wheat website (https://triticeaetoolbox.org/wheat/) and used as queries for KASP primer design using Polymarker (Ramirez-Gonzalez et al. 2015) with additional manual curation. The resulting primers (Supplementary Table 2) were used for KASP genotyping as described by Downie et al. (2018), with genomic DNA from the eight MAGIC founders extracted using a DNeasy Plant Mini Kit (Qiagen). Haplotypes were constructed using five SNPs either side of the peak marker for each QTL and markers best able to discriminate between these haplotypes selected. For QTL *QYr.niab-2D.1*, difficulties in successfully converting SNPs to KASP meant that a wider window of SNPs was considered.

Results

Analysis of YR infection in the MAGIC population

YR infection was assessed in the MAGIC population (Figure 1) grown across five trials in the UK, with phenotyping conducted at two timepoints per site. Three of the trials were conducted in 2015 (sites NIAB15, OSG15 and ROTH15) and two in 2016 (NIAB16 and OSG16). In 2016, YR scores were skewed towards the resistant end of the scoring scale, and a normal distribution was not observed. Normality for the 2016 season trials was improved using the natural log transformation, and so was used in all subsequent analyses that year. Normality tests on the 2015 season trials found the residuals to all be normally distributed, and so no further transformation was required. To account for variation within the field, three linear model approaches were applied to the 2015 raw data and the 2016 log transformed data, and the best models selected via Akaike Information Coefficient (AIC) (Supplementary Table 3). YR phenotypic data is listed in Supplementary Table 4.

Broad sense heritability was high across all test environments (h^2 = 0.93-0.95) (Supplementary Table 3). YR infection scores in the MAGIC founders spanned from 0 to 100 %, with similar trends in overall founder ranking observed between sites and years (Figure 2A). Soissons (0-3 % infection) and Robigus (70-100 % infection) were the most resistant and susceptible parents respectively, regardless of year, site and scoring timepoint. While the remaining parents varied somewhat in ranking dependent on year and location, two main founder groups were observed: relatively resistant (percentage infection range: 3-33; mean = 10.4: Alchemy, Hereward and Xi19) or relatively susceptible (percentage infection range: 17-76; mean = 36.8: Brompton, Claire and Rialto). The ranking of varieties within a trial remained the same across the two scoring timepoints. For the MAGIC RILs, YR scores were similarly distributed at the different sites within each year, but differed considerably between years (Figure 2B). In the RILs, transgressive segregation was observed in 2015 and 2016, both above and below that observed for the most susceptible and resistant founders, respectively (Figure 2B). In 2015, as YR progressed through the season and susceptibility increased among the MAGIC population, a subset of 31 RILs remained highly resistant (%inf <1) at all three sites. Intermediate YR scores (10-80 %inf) were normally distributed, with this trend more evident at OSG15 and ROTH15, where *Pst* developed more gradually compared to at NIAB15. In 2016, percent YR infection was more skewed towards resistance, compared to the previous year. High levels of resistance (%inf <1) were maintained by 32 RILs, of which eight were the same as in 2015. Overall, 121

and 171 MAGIC lines exhibited a resistant response (%inf <10) throughout the 2015 and 2016 scoring seasons respectively, at all three locations.

Genetic mapping of yellow rust resistance in MAGIC

Overall, 14 YR adult plant resistance QTL we identified (Table 2). These could be broadly divided into two groups: eight 'major' QTL that explained >5% of the phenotypic variance, were highly significant (p>1.0E-05) and identified in all trial/score combinations, and six 'minor' QTL that explained less than 5% of the variance and had lower significance (p<1.0E-05) (Tables 3-4). The eight 'major' QTL were robustly replicated, identified in all five test environments. While six of these 'major' QTL were identified via three or more genetic analysis methods, *QYr.niab-2A.2* and *QYr.niab-6A.2* were identified using IBS and IBD alone. By far the most significant QTL were located on the long arms of chromosomes 2B (*QYr.niab-2B.1*) and 2D (*QYr.niab-2D.1*) (Figure 3; Table 3), each of which had minimum p-values <2.22e^{-16} and explained up to ~18 % of the phenotypic variance. Predicted allelic effects at *QYr.niab-2B.1* showed Soissons to carry the most resistant allele, while for *QYr.niab-2D.1*, Alchemy and Claire alleles conferred the highest resistance (Table 4). The four 'major' QTL on chromosomes 1A, 2A and 3A, were found to be the next most significant YR resistance loci, with p-values ≤1.41e^{-07}. Of these, the founders Claire and Hereward conferred the strongest resistance at *QYr.niab-1A.1*, Rialto and Xi19 at *QYr.niab-2A.1*, and Hereward and Rialto at *QYr.niab-3A.1* (Table 4). As *QYr.niab-2A.2* and *QYr.niab-6A.2* were detected using single marker analysis only, no founder effects were calculated. The two remaining 'major' QTL were located on chromosome 6A, had p-values ≤1.22e^{-05}, and explained lower amounts (~5-6%) of the phenotypic variance. At *QYr.niab-6A.1*, Xi19 conferred the most resistant allele, while for *QYr.niab-6B.1* alleles from Brompton, Rialto and Xi19 conferred resistance.

Additionally, six 'minor' QTL were identified, located on chromosomes 3D (*QYr.niab-3D.1*), 4B (*QYr.niab-4B.1*), 4D (*QYr.niab-4D.1*), 5A (*QYr.niab-5A.1*), 6A (*QYr.niab-6A.3*) and 6B (*QYr.niab-6B.1*) (Table 3). These each explained a relatively low percentage of the phenotypic variance, ranging from 2.49 to 4.08%. The majority of these 'minor' QTL were detected in lower numbers of test environments, although *QYr.niab-6A.3* was detected in all but one site/score combinations analysed. *QYr.niab-4B.1* was only detected in the 2016 season trials and was the only one of the 14 YR QTL identified not to have been replicated between the two seasons.

Pairwise QTL interactions

MAGIC RILs were divided into 16 different groups, based on the presence or absence of resistance alleles at the four most significant YR QTLs (p<0.0001, PVE>8 %: *QYr.niab-1A.1, QYr.niab-2A.1, QYr.niab-2B.1* and *QYr.niab-2D.1*) (Figure 4). For each QTL, calling of the resistant allele was based on the allelic state of the consensus peak markers for each MAGIC founder. A one-way ANOVA found significant differences in the YR disease severity between all the resulting QTL combinations (p<2.2E^{-16}, Table 5). This analysis was followed by a pairwise *t*-test for the comparison of % disease severity means (Supplementary Table 5). Stacking resistance alleles at all three-way QTL combinations were among the most effective in significantly reducing MAGIC RIL YR infection and displayed high resistance responses to YR infection (*t*-test values <2.0E^{-16}). Notably, combining resistance alleles at *QYr.niab-1A.1*, *QYr.niab-2B.1* and *QYr.niab-2D.1* conferred near complete resistance across all trial sites (Figure 4). Where resistance at *QYr.niab-2D.1* was combined with resistance from *QYr.niab-1A.1* or *QYr.niab-2B.1*, the resulting two-way combinations showed significant reductions in YR susceptibility, comparable to some of the three-way combinations (*t*-test values <2.0E^{-16}). All other combinations were also significant in reducing disease severity (4.8E^{-16} <*t*-test values >2.4E^{-15}). Single QTL still provided significant levels of resistance against YR but were less effective compared to combinations (*QYr.niab-2D.1*: *t*-test value=1.3E^{-13}, *QYr.niab-1A.1*: *t*-test value=4.3E^{-10} and *QYr.niab-2A.1*: *t*-test value=1.8E^{-05}). The combination of *QYr.niab-1A.1* and *QYr.niab-2B.1* was the only one found to not significantly reduce disease severity (*t*-test value=0.04). Year and site effects were observed for the QTL combinations *QYr.niab-1A.1/QYr.niab-2A.1* and *QYr.niab-1A.1/QYr.niab-2B.1*. In both cases, the 2016 trial sites exhibited a narrower range of disease severity response compared to the 2015 sites. Similarly, the *QYr.niab-2A.1/QYr.niab-2B.1* combination was less effective in conferring YR resistance at OSG15 compared to the other trial sites. Notably, the 82 highly YR resistant MAGIC RILs (disease severity <10%) resistant across all trial sites exhibited all of the 16 QTL combinations investigated, apart from the four-way combination (1A, 2A, 2B, 2D) and *QYr.niab-1A.1* present alone.

Analysis of physical map locations of yellow rust resistance QTL

Anchoring QTL flanking markers to the wheat reference genome found the physical intervals of the eight major and minor YR QTL identified to range from 9.852 Mbp for *QYr.niab-3A.1* to 133.909 Mbp for *QYr.niab-2A.1* (median = 19.839 Mbp) (Supplemental Table 6). To investigate the genomic locations these QTL further, scatterplots of genetic (Gardner et al.

2016) versus physical (IWGSC, 2018) map locations were created for the six relevant chromosomes (1A, 2A, 2B, 2D, 3A, 6A), and the locations of the peak SNPs for each QTL highlighted (Figure 5). While at least half of each of these six chromosomes were located in regions of very low genetic recombination spanning the centromere, all eight major YR resistance QTL were located outside of these regions. Indeed, three of the eight major QTL were located <18 Mbp from the chromosome telomeres in regions with high genetic recombination (*QYr.niab-2A.2, QYr.niab-2D.1* and *QYr.niab-6A.1*), two were located on the shoulders of the non-recombining regions (*QYr.niab-2A.1*, *QYr.niab-2B.1*), with the remainder located in the intervening regions within which medium levels of genetic recombination typically occur. Of note, four QTL were located in broadly homoeologous (i.e. colinear) genomic locations: the 'major' QTL *QYr.niab-2A.2* and *QYr.niab-2D.1* on the long arm of the homoeologous chromosomes 2A and 2D, respectively, and the 'major' QTL *QYr.niab-6A.2* was colinear with 'minor' QTL *QYr.niab-6B.1* (Supplementary Table 6).

Next, using the wheat reference genome assembly and gene model annotation, we investigated the genomic locations of the 14 YR QTL in respect to overall gene density, and to the density of genes belonging to the NBS-LRR gene family (Figure 6; Supplementary Table 6). Seven of the 14 QTL were located in genomic regions that contain very high numbers of genes (>95th percentile, genome wide). Additionally, four QTL were located in regions with significantly higher number of 'resistance genes', based on simple NBS-LRR gene count (>95th percentile, genome wide). Furthermore, six QTL had a significantly higher number of 'resistance genes' than expected from the QTL gene count, compared to as expected genome-wide, calculated using the binomial cumulative probability function ($P>0.05$). Details of potential candidate genes within the QTL physical intervals, based on gene model functional annotations and predicted protein domains, as well as sequence searches using the 15 wheat rust *R* genes cloned to date (Supplemental Table 7), are detailed in Supplementary Table 8. In addition to *NLR* genes characteristic of seedling resistance genes, the colinear *QYr.niab-2A.2* and *QYr.niab-2D.1* were notable for the prominence of receptor-like kinase candidate genes, which encode proteins with protein-kinase and LRR domains. Similarly, the broadly colinear *QYr.niab-6A.2* and *QYr.niab-6B.1* QTL both had high numbers of F-box/LRR domain encoding genes in additional to multiple copies of canonical NLRs, with *QYr.niab-6B.1* also containing a PK-NLR (*TraesCS6B02G099900*; although its 6A homoeologue *TraesCS6A02G093400LC* is a pseudogene and so not annotated as a PK-NLR). *QYr.niab-2B.1* was found to span the wheat reference genome gene models reported to be homologous to the cloned wheat YR resistance

genes *Yr7* and *Yr5/YrSP*, represented in the reference genome assembly of cv. Chinese Spring by gene models *TraesCS2B02G488000* and *TraesCS2B02G488600*/*TraesCS2B02G488700*, respectively. Both *Yr7* and *Yr5/SP* encode NLRs with an integrated BED domain, with three additional BED-NLR candidate genes located very close-by (*TraesCS2B02G488400*, *TraesCS2B02G734100LC* and *TraesCS2B02G48900*). With the exception of *Yr7* and *Yr5/YrSP*, none of the remaining 13 cloned wheat *R* genes, or genes with high sequence similarity to these *R* genes, were located in the QTL intervals identified here.

Development of KASP markers tagging resistant haplotypes

For the four most robust YR QTL investigated above, we used SNPs from the 90k SNP array able to discriminate resistant and susceptible haplotypes or SNPs (Supplementary Table 2) and converted these to the KASP genotyping platform (Figure 7). For *QYr.niab-1A.1*, two SNPs (*tplb0021i12_383* and *BobWhite_c44164_402*) defined three haplotypes and were successfully converted to co-dominant KASP markers. Resistant haplotypes 1A-H1_0.0 and 1A-H2_2.0 uniquely identified the resistant alleles present in Hereward and Soissons, respectively. However, as the remaining haplotype 1A-H3_2.0 was not able to discriminate between the predicted resistant allele(s) from Claire and Xi19 from the susceptible alleles conferred by the remaining four founders, we were not able to discriminate between all of the predicted alleles at the locus. For *QYr.niab-2A.1*, two SNPs were converted to co-dominant KASP markers: *BS00062679_51* and *BS00022641_51*. These defined three haplotypes at the locus, with haplotype 2A-H1_2.0 unique to the resistant alleles present in Rialto and Xi19. The remaining two haplotypes tagged susceptible founder alleles: 2A-H2_2.2 (Alchemy, Brompton, Claire, Hereward, Robigus) and 2A-H30.2 (Soissons). For *QYr.niab-2B.1*, SNP *BS00016650_51* was converted to a co-dominant KASP marker that uniquely identified the resistant allele conferred by Soissons from all remaining seven susceptible founders. Finally, for *QYr.niab-2D.1* two markers were converted to KASP, both of which were shown in the 90k SNP array data to distinguish the resistant Alchemy and Claire alleles from the remaining six susceptible founders. However, as the polymorphisms called for all three of these markers were null (unique to the resistant alleles from Alchemy and Claire) versus a SNP call (susceptible alleles from the six remaining founders), these markers assay for presence/absence variation, and are therefore dominant.

Discussion

Pst infection at the trial sites

The spread of genetically diverse exotic *Pst* races to European environments and their displacement of the previously clonal *Pst* races has resulted in sudden shifts in wheat resistance ratings. The first of these *Pst* races to be detected in Europe is termed the 'Warrior' race (www.wheatrust.org), and was characterised by several notable traits, including relatively large reductions in resistance in varieties that previously carried effective long-term adult plant resistance (Sørensen et al. 2014) and high production of sexual stage spores (teliaspores) (Rodriguez-Algaba et al. 2014) indicative of evolution from a sexual population. In 2015, a second genetically diverse *Pst* pathotype called was detected for the first time in the UK, termed the 'Kranich' race (UKCPVS 2016). This race is broadly related to the 'Warrior' group had been previously detected in continental European countries, and both races are thought to have originated from sexually recombining populations in the near-Himalayan region in Asia (Hovmøller et al. 2016). Four of our trials were inoculated with a mixture of 'Solstice' and 'Warrior' *Pst* races, while OSG16 was naturally infected. However, natural infection was especially high in the 2015 and 2016 seasons and so likely predominated the *Pst* infection of all five trials. Testing of *Pst* isolates from the two locations used in our field trials shows these locations were dominated by natural infection by the Warrior group of races in 2015 and 2016, as was the case within the wider Cambridgeshire and Lincolnshire regions (Supplementary Table 9), and mirrored across most of the UK (UKCPVS 2016; 2017). Thus natural infection was most likely predominant in all five trials for the following reasons: (1) the high natural YR infection levels in 2015 and 2016 at these trial sites, as well as across the UK). (2) At our Lincolnshire trial sites OSG and ROTH, which were included in these surveys, the Warrior group of *Pst* races dominated. (3) Our own isolate testing from the NIAB15 and ROTH15 trials. (4) Our observation of natural YR infection prior to trial inoculation, and mirroring regional reports of very high YR disease pressure starting from autumn 2015 when mild conditions allowed rapid early spread (UKCPVS 2017). Therefore, we conclude that the adult plant resistance QTL identified in the MAGIC population most likely conferred resistance at the adult plant stage to the genetically diverse *Pst* races that characterise the recent rapid shifts in the population type of this pathogen.

Yellow rust adult plant resistance genes identified in MAGIC

The adult plant YR resistance loci identified controlled a large percentage of the phenotypic variance, predominantly accounted for by four loci on chromosomes 1A, 2A, 2B and 2D. For all but the chromosome 1A QTL, we were able to develop KASP markers that uniquely identify all MAGIC founders conferring the resistant alleles from those conferring susceptible alleles. These resources will allow these strong-effect adult plant resistance QTL to be stacked in common genetic backgrounds. Our finding that in almost all cases, combining two or more of these QTL resulted in increased resistance provide experimental evidence that such stacking should be effective in providing strong genetic control for YR. While very good resistance was generally provided by stacking two QTL, in practice the use of more loci would provide increased security against future partial or full break-down of any single adult plant resistance locus. While there was no evidence for any of the 'major' QTL breaking down over the two seasons investigated, subsequent reports indicate that the resistance conferred by *QYr.niab-2D.1* has been overcome (Simon Berry, personal communication). Gradual degradation of the adult plant YR resistance historically conferred by Claire since its release in 1999 (Powell et al. 2013) can first be traced to the period following the incursion of the 'Warrior' group of *Pst* races, when in 2011-2012 Claire went from having the highest resistance score of 9 down to an intermediate score of 6 (UKCPVS 2016). Thus, while Claire's YR resistance had partially broken down, it nevertheless contained sources of resistance unaffected by at least some of the new *Pst* races present in our 2015 and 2016 seasons, but which was further eroded by the breakdown of *QYr.niab-2D.1*. Interestingly, four adult plant YR resistance QTL have been identified on chromosomes 2B, 2D and 7B in field-grown trials of a Claire X Lemhi (CxL) population grown in trials between 2003 and 2007 (Powell et al. 2013). The trials were conducted before the introduction of the Warrior type races in 2011, and Claire alleles conferred resistance at both loci. Of these, two QTL co-located with the adult plant resistance loci identified in the MAGIC population. CxL QTL *QYr.niab-2B* overlapped with MAGIC QTL *QYr.niab-2B.1* (based on the CxL physical interval defined by markers *wPt-0950* and *wPt-9190*: 685.047 – 750.121 Mbp). However, Soissons confers the most resistant allele in the MAGIC population, indicating that the underlying loci are most likely different, or that alleles with higher resistance than that conferred by Claire are present. CxL QTL *QYr.niab-2D.2* co-located with our MAGIC QTL *QYr.niab-2D.1* (based on CxL markers *EST18a* and *wmc817a*: 637.651 - 645.997 Mbp), with resistance alleles conferred by the MAGIC founders Claire and Alchemy. Notably, Alchemy has Claire in its pedigree [Alchemy = Clare x (Consort x Woodstock)] (Fradgley et al. 2019). Indeed, the haplotypes of Claire and Alchemy based on the 90k SNP data are identical across the QTL confidence interval (from SNP

520 *RFL_Contig1128_620* to *BS00010685_51*, 188.01 – 198.86 cM), indicating the resistance
521 alleles carried by MAGIC founders Claire and Alchemy are identical by descent. The absence
522 of the chromosome 2D and 7B CxL QTL in our MAGIC population may reflect changed
523 virulence profiles of the genetically diverse *Pst* races prevalent in our 2015/2016 season trials
524 compared to the CxL trials that preceded the incursion of exotic *Ptr* races. Alternatively, it is
525 possible that none of the MAGIC founders carry the susceptible allele that originated from
526 Lemhi, which is a US variety. Interestingly, a recent study using the 'NIAB Elite MAGIC'
527 population found a robust QTL conferring resistance to the necrotrophic fungal pathogen
528 *Parastagonospora nodorum* (the causal agent of Septoria nodorum blotch, SNB) located in the
529 genomic region as the major YR resistance QTL *QYr.niab-2A.1* (Lin et al. 2020). However,
530 comparison of the predicted allelic effects at these QTL finds the resistant alleles at the YR
531 QTL carried by the founders Rialto and Xi19 to be associated with susceptibility for SNB.
532 Analysis of multiple traits in the same population allows such correlations to be identified and
533 further investigated. Indeed, as noted by Scott et al. (2020), the comparatively high genetic
534 diversity and genetic recombination captured by multi-founder populations makes them well
535 suited for the genetic analysis of multiple traits within a single experimental population, thus
536 maximising the chances of identifying potential trade-offs between traits.
537
538 *Analysis of YR QTL physical intervals*
539 All QTL identified were outside of the pericentromeric regions that are characterised by low
540 genetic recombination and encompass approximately half of the wheat genome (Figure 5).
541 This, combined with high heritability of the phenotype and the strong contrasting phenotypic
542 effect of the majority of the eight 'major' resistance QTL means that it could be useful to
543 exploit the residual heterozygosity in the MAGIC RILs to create nearly isogenic lines for
544 specific QTL for subsequent fine-mapping studies. Ultimately, combining such knowledge
545 with a better understanding of the genes conferring YR susceptibility, such as the recently
546 identified branched-chain amino acid aminotransferase gene *TaBCAT1* that modulates amino
547 acid metabolism (Corredor-Moreno et al. 2021), as well as gene editing (reviewed by Kumar
548 et al. 2019), may allow future informed design and use of resistance alleles to enhance durable
549 resistance to YR and other wheat pathogens. To date, just four YR adult plant resistance genes
550 have been map-based cloned: *Yr15/YrG303/YrH52* (Klymiuk et al. 2018; 2020), *Yr18/Lr34*
551 (Krattinger et al. 2009), *Yr36* (Fu et al. 2009), *Yr46/Lr67* (Moore et al. 2015). However, *Yr5* is
552 known to confer resistance to a broad range of *Pst* isolates worldwide (Marchal et al. 2018).
553 *Yr5* is located in a region of chromosome 2B known to contain numerous yellow rust resistance

554 genes (Feng et al. 2015; Luo et al. 2009), including *Yr7* and *YrSP*. Here we find the physical
555 interval of our MAGIC adult plant resistance locus *QYr.niab-2B.1* to overlap with the *Yr7* and
556 *Yr5/YrSp* loci. While *Yr7* and *YrSP* no longer provide adequate resistance in the field, *Yr5*
557 continues to remain effective against a range of isolates worldwide (Marchal et al. 2018). *Yr7*
558 and *Yr5* (represented in the wheat reference genome by gene models *TraesCS2B01G488000*
559 and *TraesCS2B01G488600*/*TraesCS2B01G488700*, respectively) are paralogous BED-NLR
560 genes with ~78% DNA identity across their coding regions (Marchal et al. 2018). *YrSP*
561 however is a truncated allele of *Yr5* resulting in the loss of most of the LRR coding region
562 (Marchal et al. 2018). The resistant *Yr5* and *YrSP* alleles are not reported to be present in
563 European wheat, with *Yr5/YrSP*-specific molecular tests further confirming their absence in all
564 eight MAGIC founder varieties (Marchal et al. 2018). However, previous analysis of available
565 wheat genome sequence assemblies have shown that while the cultivars Claire and Robigus
566 (two of our eight MAGIC founders) lack *Yr7*, they do contain haplotypes at the gene underlying
567 *Yr5* that encode proteins that differ by 12 and 33 amino acids to the YR resistant *Yr5* allele,
568 respectively (Marchal et al. 2018). However, neither Claire nor Robigus were reported as
569 showing the *Yr5/YrSP* resistance response, indicating these changes in the protein do not affect
570 function. In our MAGIC population, resistance at QTL *QYr.niab-2B.1* came from the Soissons
571 allele. Collectively, this indicates that while *Yr7* and *Yr5/YrSP* do not themselves confer
572 resistance at *QYr.niab-2B.1*, it is possible that different mutations at their underlying genes, or
573 allelic variation at the three additional paralogous BED-NLRs in the vicinity, could underly
574 resistance at this locus. Ultimately, further investigation of these, and other, candidates at the
575 QTL is required to narrow down the underlying causative gene and polymorphism.
576
577 *Conclusions*
578 Since 2011, several genetically diverse *Pst* races have spread rapidly across Europe from their
579 centre of origins in Asia. Better understanding of the genes and gene networks underlying adult
580 plant resistance in the face of such isolates will help breeding for YR resistance. Collectively,
581 the genetic information, wheat germplasm and molecular markers generated here provide
582 resource that could be used to help design and develop wheat varieties with improved adult
583 plant genetic resistance to emerging races of yellow rust.

Declarations

Funding: LB was funded via a Biotechnology and Biological Sciences Research Council (BBSRC) Doctoral Training Partnership PhD award to the University of Cambridge. LB also received funding from the Roger Harrison Trust towards travel expenses. JC's time was partly supported by BBSRC grant BB/N00518X/1, funded via the 2nd call of the ERA-CAPs framework.

Conflicts of interest: the authors declare no conflict of interests.

Availability of data and material: Phenotypic data is available in the Supplementary Materials. Germplasm for the 'NIAB Elite MAGIC' population is available via https://www.niab.com/research/agricultural-crop-research/resources.

Code availability: not applicable.

Author contributions: LB carried out trial preparation, pathology work, yellow rust assessments and all statistical and genetic analyses. SB and PW managed the trials at Osgodby and Rothwell. LB, CM, LP and JC undertook bioinformatics. LB and JC developed KASP markers. IM, SH and JC provided project supervision and resources. LB and JC wrote the manuscript. All authors edited and approved the manuscript.

Ethics approval: not applicable.

Consent to participate: not applicable.

Consent for publication: all authors give consent.

Acknowledgements: We thank Prof Julian Hibberd (University of Cambridge) for supervisory inputs within the Doctoral Training Programme, Keith Gardner (NIAB) for quantitative genetics advice, and the NIAB Trials Team for the sowing, growth and agronomic care of the NIAB field trails. We also thank Marie Gantet, Trynstje Broesma, Aurélie Jouanin and Doriane Dam for their support with yellow rust assessments.

References

Akaike H (1974) A new look at the statistical model identification. IEEE Trans Automat Contr 19:716–723

Alaux M, Rogers J, Letellier T, Flores R, Alfama F, Pommier C, Mohellibi N, Durand S, Kimmel E, Michotey C, Guerche C, Loaec M, Lainé M, Steinbach D, Choulet F, Rimbert H, Leroy P, Guilhot N, Salse J, Feuillet C; International Wheat Genome Sequencing Consortium, Paux E, Eversole K, Adam-Blondon AF, Quesneville H (2018) Linking the International Wheat Genome Sequencing Consortium bread wheat reference genome sequence to wheat genetic and phenomic data. Genome Biol 19:111.

Ali S, Gladieux P, Leconte M, Gautier A, Justesen AF, et al. (2014) Origin, migration routes and worldwide population genetic structure of the wheat yellow rust pathogen *Puccinia striiformis* f.sp. *tritici*. PLoS Pathol 10:e1003903.

Ali S, Rodriguez-Algaba J, Thach T, Sørensen CK, Hansen JG, Lassen P, Nazari K, Hodson DP, Justesen AF, Hovmøller MS (2017) Yellow rust epidemics worldwide were caused by pathogen races from divergent genetic lineages. Front Plant Sci 8:1057.

Altschul SF, Gish W, Miller W, Myers EW, Lipman DJ (1990) Basic local alignment search tool. J Mol Biol 215:403-410.

Andersen EJ, Nepal MP, Purintun JM, Nelson D, Mermigka G, Sarris PF (2020) Wheat disease resistance genes and their diversification through integrated domain fusions. Front Genet 11:898.

Andersson MX, Kourtchenko O, Dangl JL, Mackey D, Ellerström M (2006) Phospholipase-dependent signalling during the AvrRpm1- and AvrRpt2-induced disease resistance responses in *Arabidopsis thaliana*. Plant J 47:947–59.

Arora S, Steuernagel B, Gaurav K, Chandramohan S, Long Y, et al. (2019) Resistance gene cloning from a wild crop relative by sequence capture and association genetics. Nature Biotechnol 37:139-143.

Axtell MJ, Chisholm ST, Dahlbeck D, Staskawicz BJ (2003) Genetic and molecular evidence that the *Pseudomonas syringae* type III effector protein AvrRpt2 is a cysteine protease. Mol Microbiol 49:1537–1546 .

Bates D, Mächler M, Bolker B, Walker S (2015) Fitting linear mixed-effects models using lme4. J Stat Softw 67:1-48. doi: 10.18637/jss.v067.i01.

Bayles R, Flath K, Hovmøller M, de Vallavieille-Pope C (2000) Breakdown of the *Yr17* resistance to yellow rust of wheat in northern Europe. Agronomie 20:805-811.

Brueggeman R, Rostoks N, Kudrna D, Kilian A, Han F, Chen J, Druka A, Steffenson B, Kleinhofs A (2002) The barley stem rust-resistance gene *Rpg1* is a novel disease-resistance gene with homology to receptor kinases. Proc Natl Acad Sci USA 99:9328-9333.

Bueno-Sancho V, Persoons A, Hubbard A, Cabrera-Quio LE, Lewis CM, Corredor-Moreno P, Bunting DCE, Ali S, Chng S, Hodson DP, Burrows RM, Bryson R, Thomas J, Holdgate S, Saunders DGO (2017) Pathogenomic analysis of wheat yellow rust lineages detects seasonal variation and host specificity. Genome Biol Evol 9:3282-3296.

Chen W, Wellings C, Chen X, Kang Z, Liu T (2014) Wheat stripe (yellow) rust caused by *Puccinia striiformis* f sp. *tritici*. Mol Plant Pathol 15:433-446.

Cockram J, Mackay I (2018) Genetic mapping populations for conducting high-resolution trait mapping in plants. In: Varshney R, Pandey M, Chitikineni A (eds) Plant genetics and molecular biology. Advances in Biochemical Engineering/Biotechnology, vol 164. Springer, Cham.

Corredor-Moreno P, Minter F, Davey PE, Wegel E, Kular B, Brett P, Lewis CM, Morgan YML, Macías Pérez A, Lorolev AV, Hill L, Saunders DGO (2021) The branched-chain amino acid aminotransferase TaBCAT1 modulates amino acid metabolism and positively regulates wheat rust susceptibility. Plant Cell https://doi.org/10.1093/plcell/koab049.

Corsi B, Percival-Alwyn L, Downie RC, Venturini L, Holdgate S, Iagallo EM, Mantello CC, McCormick-Barnes C, See PT, Oliver RP, Moffat CS, Cockram J (2020) Genetic analysis of

685 wheat sensitivity to the ToxB fungal effector from *Pyrenophora tritici-repentis,* the causal
686 agent of Tan Spot. Theor Appl Genet 133:939-950.
687
688 Downie RC, Bouvet L, Furuki E, Gosman N, Gardner KA, Mackay IJ, Mantello CC, Mellers
689 G, Phan HTT, Rose GA, Tan K-C, Oliver RP, Cockram J (2018) Assessing European wheat
690 sensitivities to *Parastagonospora nodorum* necrotrophic effectors and fine-mapping of the
691 *Snn3-B1* locus conferring sensitivity to the effector SnTox3. Front Plant Sci 9:881.
692
693 Downie RC, Lin M, Borsi B, Ficke A, Lillemo M, Oliver RP, Phan H, Tan K-C, Cockram J
694 (2020) Spetoria nodorum blotch of wheat: disease management and resistance breeding in the
695 face of shifting disease dynamics and a changing environment. Phytopathol doi:
696 https://doi.org/10.1094/PHYTO-07-20-0280-RVW.
697
698 Edmondson RN (2020) Multi-level block designs for comparative experiments. J Agr Biol
699 Envir St 25:500-522.
700
701 Fragley N, Gardner KA, Cockram J, Elderfield J, Hickey JA, Howell P, et al. (2019) A large-
702 scale pedigree resource of wheat reveals evidence for adaptation and selection by breeders.
703 PLOS Biol 17:e3000071.
704
705 Fu D, Uauy C, Distelfeld A, Bechl A, Epstein L, Chen X, Sela H, Fahima T, Dubcovsky J
706 (2009) A novel kinase-START gene confers temperature-dependent resistance to wheat stripe
707 rust. Science 322:1357-1360.
708
709 Gardner KA, Wittern LM, Mackay IJ (2016) A highly recombined, high-density, eight founder
710 wheat MAGIC map reveals extensive segregation distortion and genomic locations of
711 introgression segments. Plant Biotechnol J 14:1406-1417.
712
713 He H, Zhu S, Zhao R, Jiang Z, Ji Y, Ji J, Qiu D, Li H, Bie T (2018) *Pm21,* encoding a typical
714 CC-NBS-LRR protein, confers broad-spectrum resistance to wheat powdery mildew disease.
715 Mol Plant 11:879-882.
716
717 Huang BE, George AW (2011) R/mpMap: a computational platform for the genetic analysis of
718 multiparent recombinant inbred lines. Bioinformatics 27:727-729.

Hubbard A, Lewis C, Yoshida K, Ramirez-Gonzalez R, de Vallavieille-Pope C, Thomas J, Kamoun S, Bayles R, Uauy C, Saunders DG (2015) Field pathogenomics reveals the emergence of a diverse wheat yellow rust population. Genome Biol 16:23.

Hurni S, Brunner S, Buchmann G, Herren G, Jordan T, Krukowski P, Wicker T, Yahiaoui Nm Mago R, Keller B (2013) Rye *Pm8* and wheat *Pm3* are orthologous genes and show evolutionary conservation of resistance function against powdery mildew. Plant J 76:957-969.

Hovmøller MS, Walter S, Bayles RA, Hubbard A, Flath K, Sommerfeldt N, Leconte M, Czembor P, Rodriguez-Algaba J, Thach T, Hansen JG, Lassen P, Justesen AF, Ali S, de Vallavieille-Pope C (2016) Replacement of the European wheat yellow rust population by new races from the centre of diversity in the near-Himalayan region. Plant Pathol 65:402-411.

Hubbard A, Lewis C, Yoshida K, Ramirez-Gonzalez R, de Vallavieille-Pope C, Thomas J. et al. (2015) Field pathogenomics reveals the emergence of a diverse wheat yellow rust population. Genome Biol 16:23.

The International Wheat Genome Sequencing Consortium (IWGSC), Appels R, Eversole K, Stein N, Feuillet C, Keller B, Rogers J Pozniak C, et al. (2018) Shifting the limits in wheat research and breeding using a fully annotated reference genome. Science 361:eaar7191.

Jamil S, Shahzad R, Ahmad S, Fatima R, Zahid R, Anwar M, Iqbal MZ, Wang X (2020) Role of genetics, genomics and breeding approaches to combat stripe rust of wheat. Front Nutr 7:580715.

Jones JD, Vance RE, Dangl JL (2016) Intracellular innate immune surveillance devices in plants and animals. Science 354:aaf6395.

Kertho A, Mamidi S, Bonman JM, McClean PE, Acevedo M (2015) Genome-wide association mapping for resistance to leaf and stripe rust in winter-habit hexaploid wheat landraces. PLoS ONE 10:e0129580.

752 Klymiuk V, Taniv E, Huang L, Raats D, Fatiukha A, et al. (2018) Cloning of the wheat *Yr15*
753 resistance gene sheds light on the plant tandem kinase-pseudokinase family. Nat Commun
754 9:3735.
755
756 Klymiuk V, Fatiukha A, Raats D, Bocharova V, Huang L, Feng L, Jaiwar S, Pozniak Cm
757 Coaker G, Dubcovsky J, Fahima T (2020) Three previously characterized resistances to
758 yellow rust are encoded by a single locus *Wtk1*. J Exp Bot 71:2561-2572.
759
760 Krzywinski M, Schein J, Birol I, Connors J, Gascoyne R, Horsman D, Jones SJ, Marra MA
761 (2009) Circos: an information aesthetic for comparative genomics. Genome Res 19:1639-45.
762
763 Kumar R, Kaur A, Pandey A, Mamrutha HM, Singh GP (2019) CRISPR-based genome
764 editing in wheat: a comprehensive review and future prospects. Mol Biol Rep 46:3557-3569.
765
766 Li M, Dong L, Li B, Wang Z, Xie J, et al. (2020) A CNL protein in wild emmer wheat confers
767 powdery mildew resistance. New Phytol 228:1027-1037.
768
769 Lin M, Corsi B, Ficke A, Tan K-C, Cockram J, Lillemo M (2020) Genetic mapping using a
770 wheat multi-founder population reveals a locus on chromosome 2A controlling resistance to
771 both leaf and glume blotch caused by the necrotrophic fungal pathogen *Parastagonospora*
772 *nodorum*. Theor Appl Genet 133:785-808.
773
774 Loutre C, Wicker T, Travella S, Galli P, Scofield S, Fahima T, Feuillet C, Keller B (2009)
775 Two different CC-NBS-LRR genes are required for *Lr10*-mediated leaf rust resistance in
776 tetraploid and hexaploid wheat. Plant J 60:1043-1054.
777
778 Luo PG, Hu XY, Ren ZL, Zhang HY, Shu K, Yang ZJ (2008) Allelic analysis of stripe rust
779 resistance genes on wheat chromosome 2BS. Genome 51:922–927.
780
781 Mackay TF (2001) The genetic architecture of quantitative traits. Annu Rev Genet 35:303–
782 339.
783
784 Maccaferri M, Zhang J, Bulli P, Abate Z, Chao S, Cantu D, Bossolini E, Chen X, Pumphrey
785 M, Dubcovsky J (2015) A genome-wide association study of resistance to stripe rust (*Puccinia*

striiformis f. sp. *tritici*) in a worldwide collection of hexaploid spring wheat (*Triticum aestivum* L.). G3: Genes, Genomes, Genet 5:449–465.

Mackay IJ, Bansept-Basler P, Barber T, Bentley AR, Cockram J, Gosman N, Greenland AJ, Horsnell R, Howells R, O'Sullivan DM, Rose GM, Howell PH (2014) An eight-parent multiparent advanced generation inter-cross population for winter sown wheat: creation, properties, and validation. G3: Genes Genomes Genet 4:1603–1610.

Mackey D, Holt 3rd BF, Wiig A, Dangl JL (2002) RIN4 interacts with *Pseudomonas syringae* type III effector molecules and is required for RPM1-mediated resistance in *Arabidopsis*. Cell 108:743–54.

Marchal C, Zhang J, Zhang P, Fenwick P, Steuernagel B, Adamski NM, Boyd L, McIntosh R, Wulff BBH, Berry S, Lagudah E, Uauy C (2018) BED-domain-containing immune receptors confer diverse resistance spectra to yellow rust. Nature Plants 4:662–668.

Milus EA, Kristensen K, Hovmøller MS (2009) Evidence for increased aggressiveness in a recent widespread strain of *Puccina striiformis* f. sp. *tritici* causing stripe rust of wheat. Phytopathol 99:89-94.

Peterson RF, Campbell AB, Hannah AE (1948) A diagrammatic scale for estimating rust intensity on leaves and stems of cereals. Can J Res 26c:496–500.

Powell NM, Lewis CM, Berry ST, MacCormack R, Boyd LA (2013) Stripe rust resistance genes in the UK winter wheat cultivar Claire. Theor Appl Genet 126:1599-1612.

R Core Team (2013) R: A language and environment for statistical computing. R Foundation for Statistical Computing, Vienna, Austria. URL http://www.R-project.org/.

Ramirez-Gonzalez R, Uauy C, Caccamo M (2015) PolyMarker: A fast polyploid primer design pipeline. Bioinformatics 31:2038–2039.

818 Rodriguez-Algaba J, Walter S, Sørensen CK, Hovmøller MS, Justesen AF (2014) Sexual
819 structures and recombination of the wheat rust fungus *Puccinia striiformis* on *Berberis*
820 *vulgaris*. Fungal Genet Biol 70:77–85.
821
822 Rosewarne GM, Herrera-Foessel SA, Singh RP, Huerta-Espino J, Lan CX, He ZH (2013)
823 Quantitative trait loci of stripe rust resistance in wheat. Theor Appl Genet 126:2427–2449.
824
825 Sánchez-Martin J, Steuernagel B, Ghosh S, Herren G, Hyrni S, et al. (2016) Rapid gene
826 isolation in barley and wheat by mutant chromosome sequencing. Genome Biol 17:221.
827
828 Sarris P, Cevik V, Dagadas G, Jones JDG, Krasileva KV (2016) Comparative analysis of plant
829 immune receptor architectures uncovers host proteins likely targeted by pathogens. BMC Biol
830 14:8.
831
832 Scott M, Ladejobi O, Sammer A, Bentely AR, Biernaskie J, Bowden SA, Dell'Acqua M,
833 Dixon LE, Filippi CV, Fradgley N, Gardner KA, Mackay IJ, O'Sullivan D, Percival-Alwyn
834 L, Roorkiwal M, Singh RK, Thudi M, Varshney RK, Venturini L, Whan A, Cockram J, Mott
835 R (2020) Multi-parent populations in crops: a toolbox integrating genomics and genetic
836 mapping with breeding. Heredity 125:396-416.
837
838 Singh RP, Huerta-Espino J, William HM (2005) Genetics and breeding for durable resistance
839 to leaf and stripe rusts in wheat. *In*: Turkish J Agric Forestry 29:121–127.
840
841 Sørensen CK. Hovmøller MS, Leconte M, Dedryver F, de Vallavieille-Pope C (2014) New
842 races of *Puccina striiformis* found in Europe reveal race specificity of long-term effective adult
843 plant resistance in wheat. Phytotaphol 104:1042-1051.
844
845 Steuernagel B, Witek K, Krattinger SG, Ramirez-Gonzalez RH, Schoonbeek J-J, Yu G, Baggs
846 E, Witek AI, Yadav I, Krasileva KV, Jones JDG, Uauy C, Keller B, Ridout CJ, Wulff BBH
847 (2020) The NLR-annotator tool enables annotation of the intracellular immune receptor
848 repertoire. Plant Physiol https://doi.org/10.1104/pp.19.01273.
849

850 Thind AK, Wicker T, Šimková H, Fossati D, Moullet O, Brabant C, Vrána J, Doležel J,
851 Krattinger SG (2017) Rapid cloning of genes in hexaploid wheat using cultivar-specific long-
852 range chromosome assembly. Nat Biotechnol 35:793-796.
853
854 UKCPVS (2016) United Kingdom cereal pathogen virulence survey 2016 annual report.
855 https://ahdb.org.uk/ukcpvs .
856
857 VSN International (2015) Genstat for Windows. VSN International, Hemel Hempstead, 18th
858 Edition. UK webpage: www.genstat.co.uk.
859
860 Wang M, Chen X (2017) Stripe Rust Resistance. In: Chen X, Kang Z. (eds) Stripe rust.
861 Springer, Dordrecht.
862
863 Wang S, Wong D, Forrest K, Allen A, Chao S, Huang BE, et al. (2014) Characterization of
864 polyploid wheat genomic diversity using a high-density 90,000 single nucleotide
865 polymorphism array. Plant Biotechnol J 12:787–796.
866
867 Wellings CR (2011) Global status of stripe rust: a review of historical and current threats.
868 Euphytica 179:129-141.
869
870 Wilcoxon RD, Skovmand B, Atif AH (1975) Evaluation of wheat cultivars for ability to retard
871 development of stem rust. Ann Appl Biol 80:275–281.
872
873 Zadoks Z, Chang TT, Konzak CF (1974) A decimal code for the growth stages of cereals.
874 Weed Res 14:415-421.
875
876 Zegeye H, Rasheed A, Makdis F, Badebo A, Ogbonnaya FC (2014) Genome-wide association
877 mapping for seedling and adult plant resistance to stripe rust in synthetic hexaploid wheat.
878 PLoS ONE 9:e105593.
879
880 Zhang W, Chen S, Abate Z, Nirmala J, Rouse MN, Dubcovsky J (2017) Identification and
881 characterization of *Sr13*, a tetraploid wheat gene that confers resistance to the Ug99 stem rust
882 race group. Proc Natl Acad Sci U S A 114:E9483-E9492.

883 **Figure legends**

884

885 **Figure 1.** Examples of yellow rust resistance phenotypes in the MAGIC population. Assessments were made using the modified Cobb's scale
886 (Peterson et al. 1948) ranging from 0 to 100 %: (a) score=0, no infection, 0%, (b) some tillers infected with a few stripes 0-15%, (c) most tillers
887 infected with several stripes, 15-25%, (d) all leaves infected, 25-50%, (e) all leaves infected, 50-75%, (f) little to no green tissue left, >75%.

888

889 **Figure 2.** Yellow rust resistance in the MAIGC population. Five test environments: NIAB, Osgodby and Rothwell in 2015 (NIAB15, OSG15,
890 ROTH15) and at NIAB and Osgodby in 2016 (NIAB16, OSG16). At each site, YR infection was recorded at two timepoints: S1 (score 1) and S2
891 (score 2). Al = Alchemy, Br = Brompton, Cl = Claire, He = Hereward, Ri = Rialto, Ro = Robigus, So = Soissons, Xi = Xi19. (A) MAGIC founder
892 percentage YR resistance scores. Additionally, boxplots for all MAGIC recombinant inbred lines are indicated for each trial. (B) Histograms of
893 percentage YR infection in the MAGIC recombinant inbred lines (RILs). Data for the non-transformed adjusted means (BLUEs) are shown for
894 the RILs,. BLUEs for each of the eight founders are overlaid below, following the colour coding shown in the key. Note: for QTL analysis, the
895 2016 season data was log transformed. Negative values = 0. Values over 100 = 100.

896

897 **Figure 3.** Examples of yellow rust resistance genetic analysis. Shown is the NIAB15 dataset analysed using composite interval mapping with 10
898 covariates (CIM-cov10), showing QTL scans using the following phenotypes: (A) scoring time-point 1, (B) scoring time-point 1, and (C) scoring
899 time-point 2. All 21 wheat chromosomes are shown, with 1=chromosome 1A, 2=1B, 3=1D, through to 21=7D.

900

901 **Figure 4.** The effects of combining yellow rust (YR) resistance alleles at multiple QTL. Boxplots of the distribution of YR percentage infection
902 in MAGIC recombinant inbred lines (RILs) in each of the five field trials. Based on the presence of resistance alleles at up to four of the most
903 significant MAGIC YR resistance quantitative trait loci (QTL): on chromosomes 1A (*QYr.niab-1A.1*), 2A (*QYr.niab-2A.1*), 2B (*QYr.niab-2B.1*)

and 2D (*QYr.niab-2D.1*). Boxes denote the interquartile range, the horizontal lines that bisect them the median, the vertical lines that extend from them the 1.5 x interquartile range beyond it, and the dots the outlier MAGIC RILs.

Figure 5. Locations of the eight most significant yellow rust QTL visualised on plots of all genetically mapped SNPs in the MAGIC genetic map (cM) (Gardner et al. 2016) versus their physical map locations (Mbp) (IWGSC Refseq v1.0). Shown are: (A) *QYr.niab-1A.1* (represented by peak SNP *RAC875_rep_c71093_1070*) on chromosome 1A, (B) *QYr.niab-2A.1* (*BS00022903_51*) and *QYr.niab-2A.2* (*BS00011599_51*) on chromosome 2A. (C) *QYr.niab-2B.1*(*Kukri_c9118_1774*) on chromosome 2B. (D) *QYr.niab-2D.1* (*Ra_c21099_1781*) on chromosome 2D. (E) *QYr.niab-3A.1* (*Kukri_c28650_111*) on chromosome 3A. (F) *QYr.niab-6A.1* (*BS00011010_51*) and *QYr.niab-6A.2* (*Kukri_c21743_269*) on chromosome 6A.

Figure 6. Circular diagram representing the position of 14 yellow rust (YR) resistance QTL identified in the MAGIC wheat population, in relation to density of candidate 'resistance genes' present in the cv. Chinese Spring reference genome (RefSeq v1.0; IWGSC, 2018). Starting from the outermost, Track 1: chromosome number. Track 2: tick marks indicating the position of major (red) and minor (green) YR QTL. Track 3 (purple): histogram of the proportion of resistant genes per gene per 10Mbp. Track 4 (blue): histogram of 'resistant gene' count every 10 Mbp. Track 5 (dark blue): histogram of gene count every 10 Mbp.

Figure 7. Examples of genotyping results for some of the KASP markers developed for the four most significant yellow rust resistance QTL (see Supplementary Table 2 for full details). Genotype calls for resistant (Res) and susceptible (Sus) alleles are indicated, derived from genomic DNA template from the founders subsequently indicated here. NTC = no template negative control. (A) *QYr.niab-1A.1*: KASP marker *tplb0021i12_383* (DNA: Alchemy, susceptible allele; Hereward, resistant allele). (B) *QYr.niab-2A.1*: KASP marker *BS00062679_51* (DNA: Xi19, resistant allele; Claire, susceptible allele). (C) *QYr.niab-2B.1*: KASP marker *BS00016650_51* (DNA: Soissons, resistant allele; Robigus, susceptible allele). (D) *QYr.niab-2D.1*: KASP marker *Kukri_c498_2381* (DNA: Claire, resistant allele; Soissons, susceptible allele).

926

Trial	NIAB15	OSG15	ROTH15	NIAB16	OSG16
Location	Cambridge	Osgodby	Rothwell	Cambridge	Osgodby
Total number of plots	2,208	1,200	1,200	1,200	1,200
Columns x rows	48 cols x 46 rows	20 cols x 60 rows	20 cols x 60 rows	20 cols x 60 rows	20 cols x 60 rows
Main : blocks : subblocks per block	2:46:0	-	-	2:3:2	2:3:2
MAGIC RILs replicated	1,085	-	-	444	444
MAGIC RILs unreplicated	-	1,060	1,060	234	234
MAGIC founders	8	8	8	8[†]	8[†]
Varietal controls	10[a]	2[b]	2[b]	2[†]	2[†]
MAGIC founder controls	-	20[c]	20[c]	-	-
Additional checks	-	Vuka[£]	Vuka[£]	-	-

Table 1. Overview of the five yellow rust MAGIC trials undertaken in the United Kingdom during the 2015 and 2016 seasons. An unbalanced incomplete random block design was used for all trials. [a]Controls: the yellow rust differential lines Ambition (YR resistance gene *Am*), Cadenza (*Ca*), KWS Sterling (*St*), Rendezvous (*Re*), Solstice (*So*), Spaldings Prolific (*Sp*), Timber (*Ti*), Warrior (*Wa*), the positive control Vuka (-) and the negative control Cougar (*Co*). [b]Controls: Vuka (positive control) and Cougar (negative control). [c]20 MAGIC RIL lines used for controls, listed in Supplementary Table 1). All lines and controls were present as two replicates, unless otherwise stated: [†]Control varieties Oakley (positive control) and Cougar (negative control), each replicated three times. [£]Susceptible variety Vuka replicated 80 times.

QTL	Chr.	Environments									
		NIAB15		OSG15		ROTH15		NIAB16		OSG16	
A		S1	S2	S1	S2	S1	S2	S1	S2	S1	S2
QYr.niab-1A.1	1A	1-4	1-4	1-4	1-4	1-2	1-2	1-4	1-4	1-4	1-4
QYr.niab-2A.1	2A	1-4	1-4	1-4	1-4	1-4	1-4	1-4	1-4	1-4	1-4
QYr.niab-2A.2	2A	1-2	1-2	1-2	1-2	1-2	1	1-2	1-2	1	1
QYr.niab-2B.1	2B	1-4	1-4	1-4	1-4	1-4	1-4	1-4	1-4	1-4	1-4
QYr.niab-2D.1	2D	1-4	1-4	1-4	1-4	1-4	1-4	1-4	1-4	1-4	1-4
QYr.niab-3A.1	3A	1-4	1-4	1-4	1-4	1-2	1-2	2-4	3	1-4	1-4
QYr.niab-6A.1	6A	2-4	2-4	3-4	2-4	2	2	2-4	1-4	1-4	1-4
QYr.niab-6A.2	6A	1-2	1-2	1-2	1-2	1-2	1-2	1-2	1-2	1-2	1-2
B											
QYr.niab-3D.1	3D	2	2	1-2	1,2,4	1-3	1-3	2	2		
QYr.niab-4B.1	4B							1-4		1-2	
QYr.niab-4D.1	4D	1-2	2							1-4	1-3
QYr.niab-5A.1	5A	1,2,4	1,2,4			1			1		
QYr.niab-6A.3	6A	2		2	2	2	2	2	2	1-2	1-2
QYr.niab-6B.1	6B		4	1-4	1-4	2-3	2-3				

Table 2. 'Major' (**A**) and 'minor' (**B**) yellow rust resistance QTL identified in the MAGIC population using four different QTL analysis methods. QTL analysis methods are numbered as: 1 = single marker analysis, 2 = identity by descent (IBD), 3 = interval mapping, 4 = composite interval mapping with 10 covariates. Trial sites: NIAB, Osgodby (OSG), Rothwell (ROTH). Trial years: 2015 and 2016. Yellow rust resistance phenotyping was undertaken at two timepoints: score-1 (S1) and score-2 (S2). Chr. = chromosome. QTL were detected at 5 % significance threshold.

QTL	Chr.	Peak SNP marker	Genetic position (cM)	Physical position (Mbp)	*p*-value		% var. explained		QTL interval (cM)
					min	max	min	max	
QYr.niab-1A.1	1A	*RAC875_rep_c71093_1070*	185.80	568.013	5.72E-10	1.23E-05	7.46	9.26	17.17
QYr.niab-2A.1	2A	*BS00022903_51*	140.26	607.827	3.07E-13	1.24E-08	6.80	9.37	19.29
QYr.niab-2A.2	2A	*BS00011599_51*	259.39	762.290	1.75E-08	7.91E-03	-	-	2.56
QYr.niab-2B.1	2B	*Kukri_c9118_1774*	271.92	683.048	0*	1.58E-11	7.38	17.72	18.62
QYr.niab-2D.1	2D	*Ra_c21099_1781*	197.36	638.376	0*	8.62E-12	10.83	18.38	10.85
QYr.niab-3A.1	3A	*Kukri_c28650_111*	3.02	7.921	1.41E-07	5.58E-04	3.48	6.02	16.64
QYr.niab-3D.1	3D	*BS00004334_51*	162.20	574.773	3.30E-05	1.40E-03	3.35	-	0
QYr.niab-4B.1	4B	*Ra_c26080_461*	50.66	36.643	3.72E-05	-	-	2.97	17.73
QYr.niab-4D.1	4D	*D_GDRF1KQ02H66WD_341*	125.78	499.107	1.-7E-05	2.44E-04	2.89	4.03	26.56
QYr.niab-5A.1	5A	*IAAV3916*	301.25	683.343	1.21E-04	9.62E-03	3.48	3.60	13.32
QYr.niab-6A.1	6A	*BS00011010_51*	55.51	18.713	4.52E-10	1.22E-05	5.50	6.57	18.24
QYr.niab-6A.2	6A	*Kukri_c21743_269*	75.69	27.108	5.15E-10	9.84E-05	-	-	2.05
QYr.niab-6A.3	6A	*wsnp_Ex_rep_c101766_87073440*	220.32	596.521	1.49E-04	1.37E-04	-	-	17.96
QYr.niab-6B.1	6B	*BS00068615_51*	60.56	54.662	1.44E-07	1.44E-05	2.49	4.08	13.37

Table 3 Details of the 14 yellow rust (YR) resistance QTL identified in the MAGIC population in seasons 2015 and 2016. The nine 'major' QTL are highlighted in bold. Pairs of QTL located in broadly colinear positions on homoeologous chromosomes are underlined. Chr. = chromosome. Genetic map position and QTL interval are from the MAGIC genetic map (Gardner et al. 2016). Minimum (min) and maximum (max) values for *p* value and percentage phenotypic variance explained (% var explained) selected amongst all environments and QTL mapping methods. * $<2.22E^{-16}$. QTL interval based on QTL mapping method-4 (composite interval mapping, 10 covariates).

QTL	Chr	Predicted founder effects								Origin
		Al	Br	Cl	He	Ri	Ro	So	Xi	(trial, YR score)
QYr.niab-1A.1	1A	14.29	7.94	-3.67	-12.58	13.31	12.67	4.16	1	NIAB15, S2 (cov0)
QYr.niab-2A.1	2A	13.19	19.73	25.82	11.65	3.46	19.59	9.29	1	OSG15, S2 (cov10)
QYr.niab-2B.1	2B	-5.48	0.72	6.79	-6.41	-12.6	1.97	-33.82	1	NIAB15, S2 (cov10)
QYr.niab-2D.1	2D	-21.77	13.46	-16.70	-5.12	33.03	21.44	12.13	1	NIAB15, S2 (cov10)
QYr.niab-3A.1	3A	1.12	-4.78	-6.15	-16.79	-22	-5.16	-6.81	1	ROTH15, S2 (cov0)
QYr.niab-6A.1	6A	16.38	14.57	14.2	7.04	20.69	21.6	7.81	1	NIAB15, S2 (cov10)

Table 4. Predicted MAGIC founder effects at six of the eight 'major' yellow rust (YR) resistance QTL. Founder effects presented are from the 2015 trials, and correspond to the consensus marker with the most significant *p*-value identified with QTL mapping methods 2, (identity by descent), 3 (interval mapping, cov=0) or 4 (composite interval mapping, covariates = 10). For QTL mapping method 2, contributions are relative to Alchemy whereas for methods 3 and 4, they are relative to Xi19. This was calibrated by adding an arbitrary value of 1 to all founder effects. For *QYr.niab-2B.1* and *QYr.niab-2D.1*, founder effects represented are from the peak marker with the highest % variation explained. QTL identified with IBS or IBD analyses only (*QYr.niab-2A.2*, *QYr.niab-6A.2*) are not included.

	SS	df	MS	*F*	*p*
Interactions	27177.9	15	1811.9	47.2	$2.2E^{-16}$
Residuals	2377.7	62	38.4		

Table 5. Analysis of variance (ANOVA) in QTL interactions in response to yellow rust disease severity. SS = sum of squares. Df = degrees of freedom. MS = mean squares.

Figures

Figure 1

Examples of yellow rust resistance phenotypes in the MAGIC population. Assessments were made using the modified Cobb's scale (Peterson et al. 1948) ranging from 0 to 100 %: (a) score=0, no infection, 0%, (b) some tillers infected with a few stripes 0-15%, (c) most tillers infected with several stripes, 15-25%, (d) all leaves infected, 25-50%, (e) all leaves infected, 50-75%, (f) little to no green tissue left, >75%.

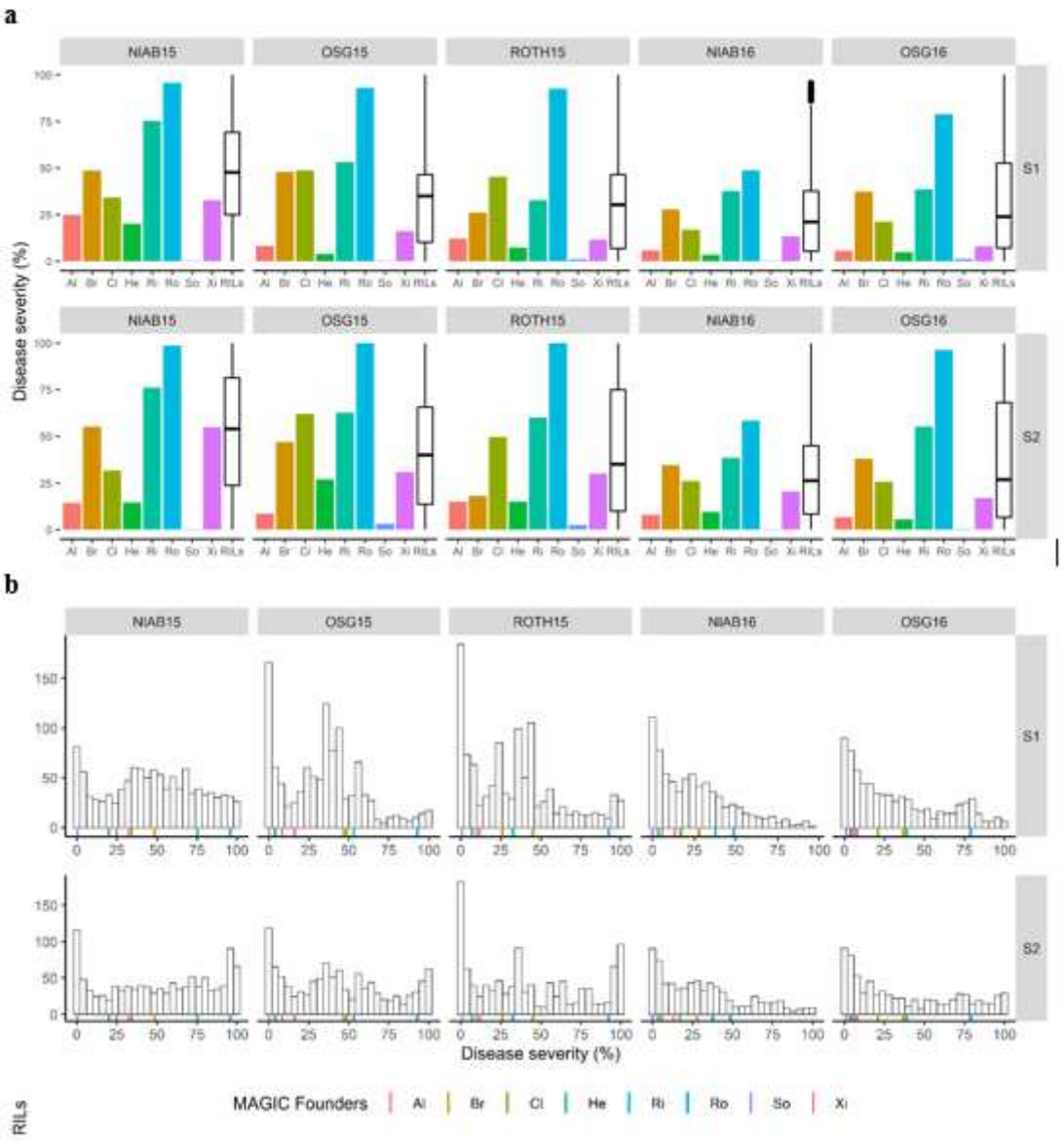

Figure 2

Yellow rust resistance in the MAIGC population. Five test environments: NIAB, Osgodby and Rothwell in 2015 (NIAB15, OSG15, ROTH15) and at NIAB and Osgodby in 2016 (NIAB16, OSG16). At each site, YR infection was recorded at two timepoints: S1 (score 1) and S2 (score 2). Al = Alchemy, Br = Brompton, Cl = Claire, He = Hereward, Ri = Rialto, Ro = Robigus, So = Soissons, Xi = Xi19. (A) MAGIC founder percentage YR resistance scores. Additionally, boxplots for all MAGIC recombinant inbred lines are indicated for each trial. (B) Histograms of percentage YR infection in the MAGIC recombinant inbred lines (RILs). Data for the non-transformed adjusted means (BLUEs) are shown for the RILs,. BLUEs for each of the eight founders are overlaid below, following the colour coding shown in the key. Note: for QTL analysis, the 2016 season data was log transformed. Negative values = 0. Values over 100 = 100.

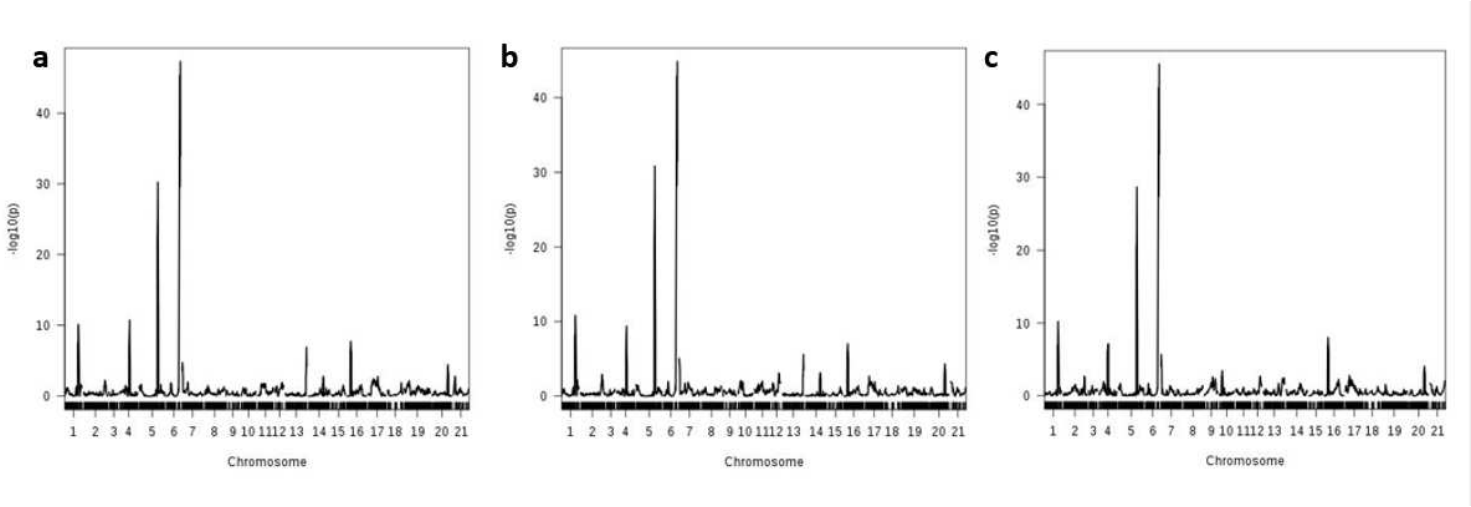

Figure 3

Examples of yellow rust resistance genetic analysis. Shown is the NIAB15 dataset analysed using composite interval mapping with 10 covariates (CIM-cov10), showing QTL scans using the following phenotypes: (A) scoring time-point 1, (B) scoring time-point 1, and (C) scoring time-point 2. All 21 wheat chromosomes are shown, with 1=chromosome 1A, 2=1B, 3=1D, through to 21=7D.

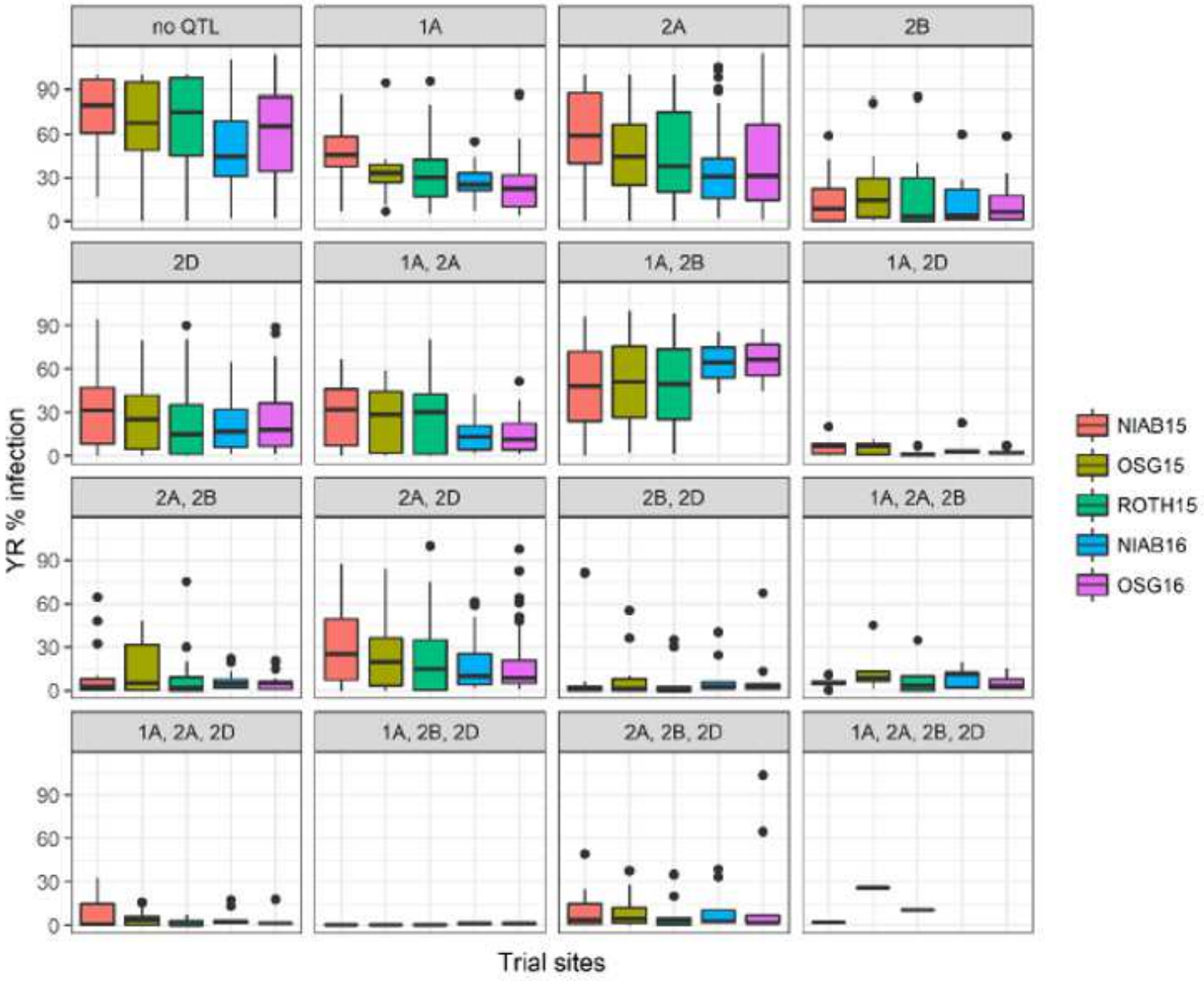

Figure 4

The effects of combining yellow rust (YR) resistance alleles at multiple QTL. Boxplots of the distribution of YR percentage infection in MAGIC recombinant inbred lines (RILs) in each of the five field trials. Based on the presence of resistance alleles at up to four of the most significant MAGIC YR resistance quantitative trait loci (QTL): on chromosomes 1A (QYr.niab-1A.1), 2A (QYr.niab-2A.1), 2B (QYr.niab-2B.1) and 2D (QYr.niab-2D.1). Boxes denote the interquartile range, the horizontal lines that bisect them the median, the vertical lines that extend from them the 1.5 x interquartile range beyond it, and the dots the outlier MAGIC RILs.

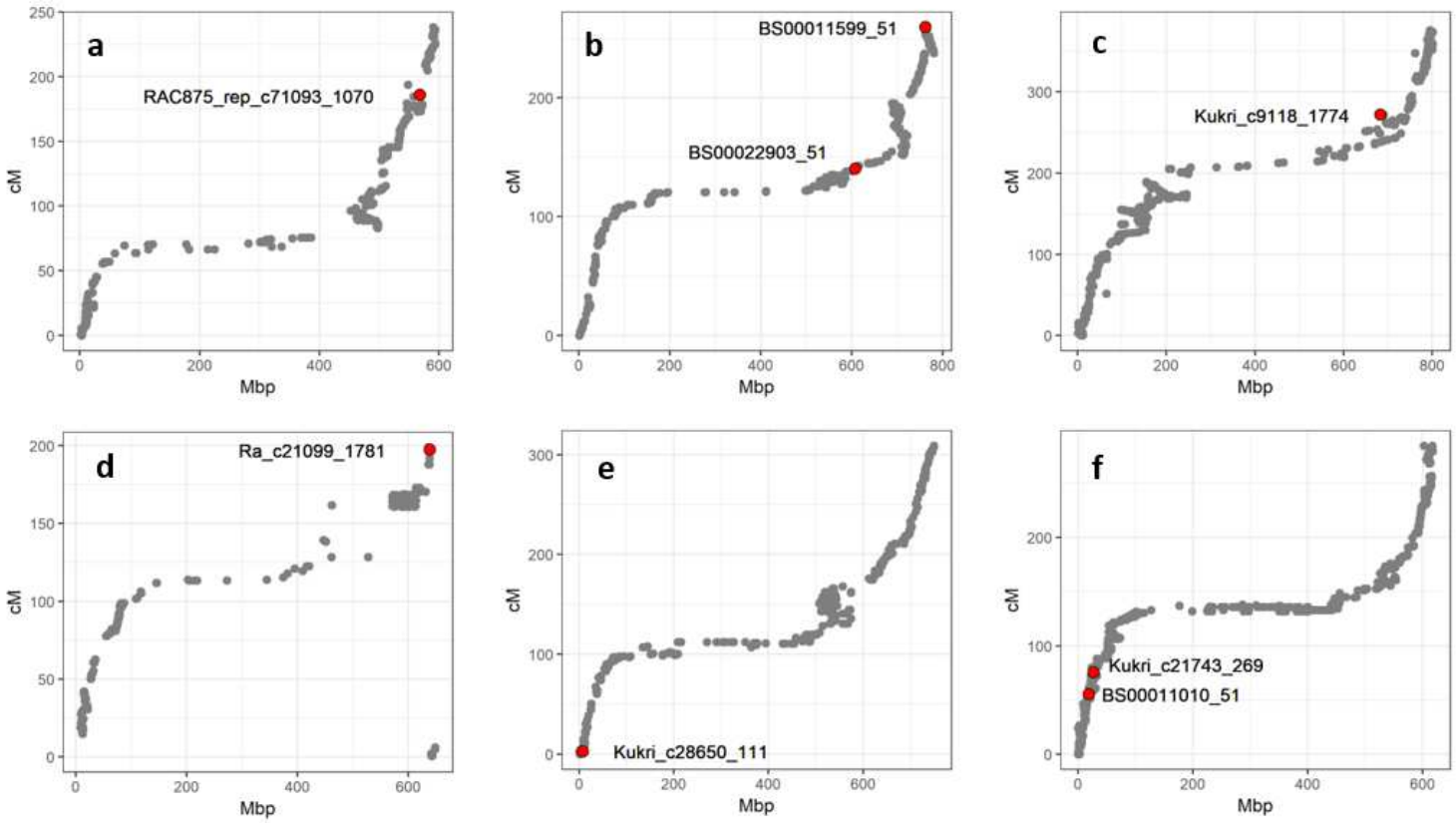

Figure 5

Locations of the eight most significant yellow rust QTL visualised on plots of all genetically mapped SNPs in the MAGIC genetic map (cM) (Gardner et al. 2016) versus their physical map locations (Mbp) (IWGSC Refseq v1.0). Shown are: (A) QYr.niab-1A.1 (represented by peak SNP RAC875_rep_c71093_1070) on chromosome 1A, (B) QYr.niab-2A.1 (BS00022903_51) and QYr.niab-2A.2 (BS00011599_51) on chromosome 2A. (C) QYr.niab-2B.1(Kukri_c9118_1774) on chromosome 2B. (D) QYr.niab-2D.1 (Ra_c21099_1781) on chromosome 2D. (E) QYr.niab-3A.1 (Kukri_c28650_111) on chromosome 3A. (F) QYr.niab-6A.1 (BS00011010_51) and QYr.niab-6A.2 (Kukri_c21743_269) on chromosome 6A.

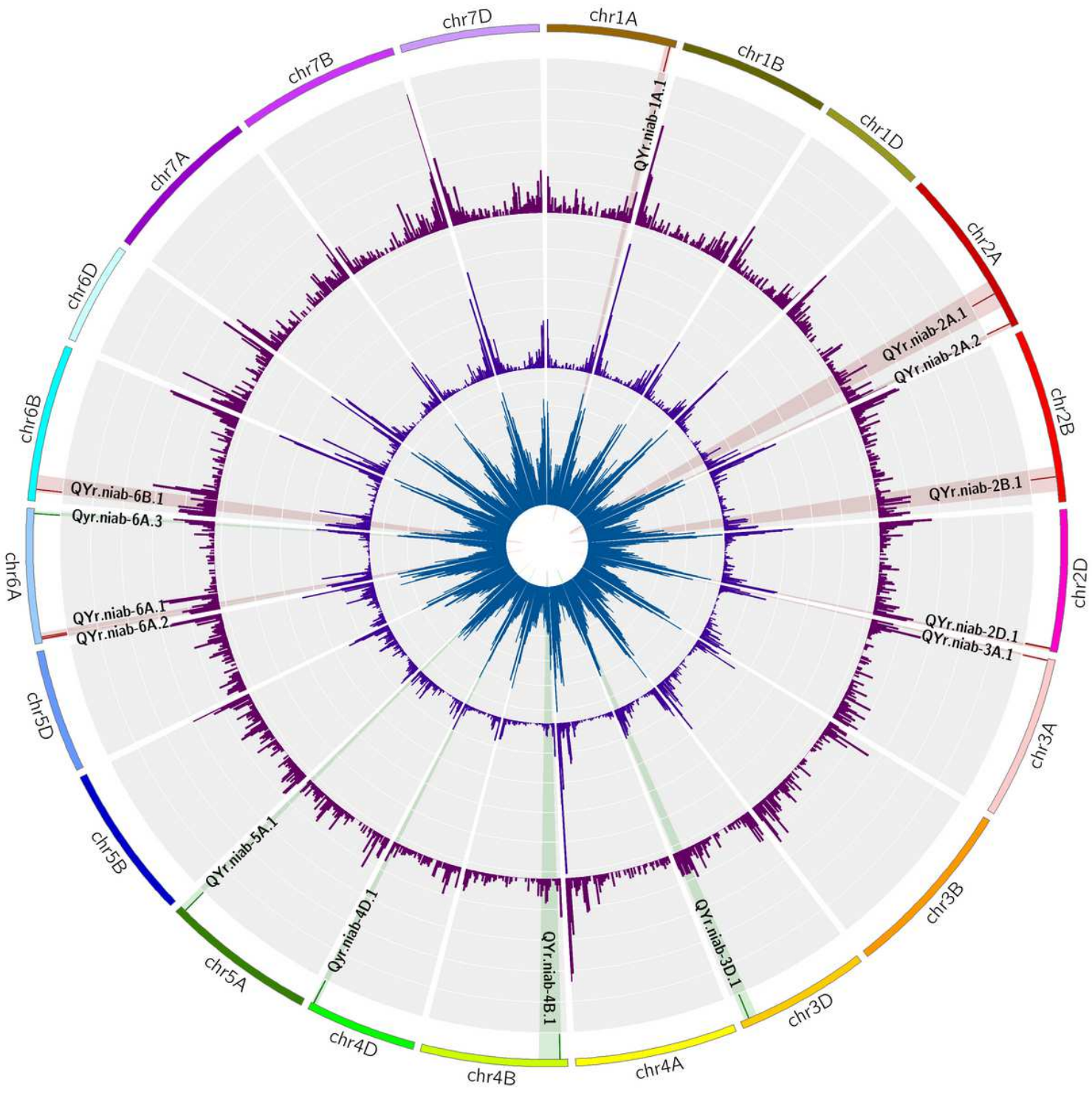

Figure 6

Circular diagram representing the position of 14 yellow rust (YR) resistance QTL identified in the MAGIC wheat population, in relation to density of candidate ‘resistance genes’ present in the cv. Chinese Spring reference genome (RefSeq v1.0; IWGSC, 2018). Starting from the outermost, Track 1: chromosome number. Track 2: tick marks indicating the position of major (red) and minor (green) YR QTL. Track 3 (purple): histogram of the proportion of resistant genes per gene per 10Mbp. Track 4 (blue): histogram of ‘resistant gene’ count every 10 Mbp. Track 5 (dark blue): histogram of gene count every 10 Mbp.

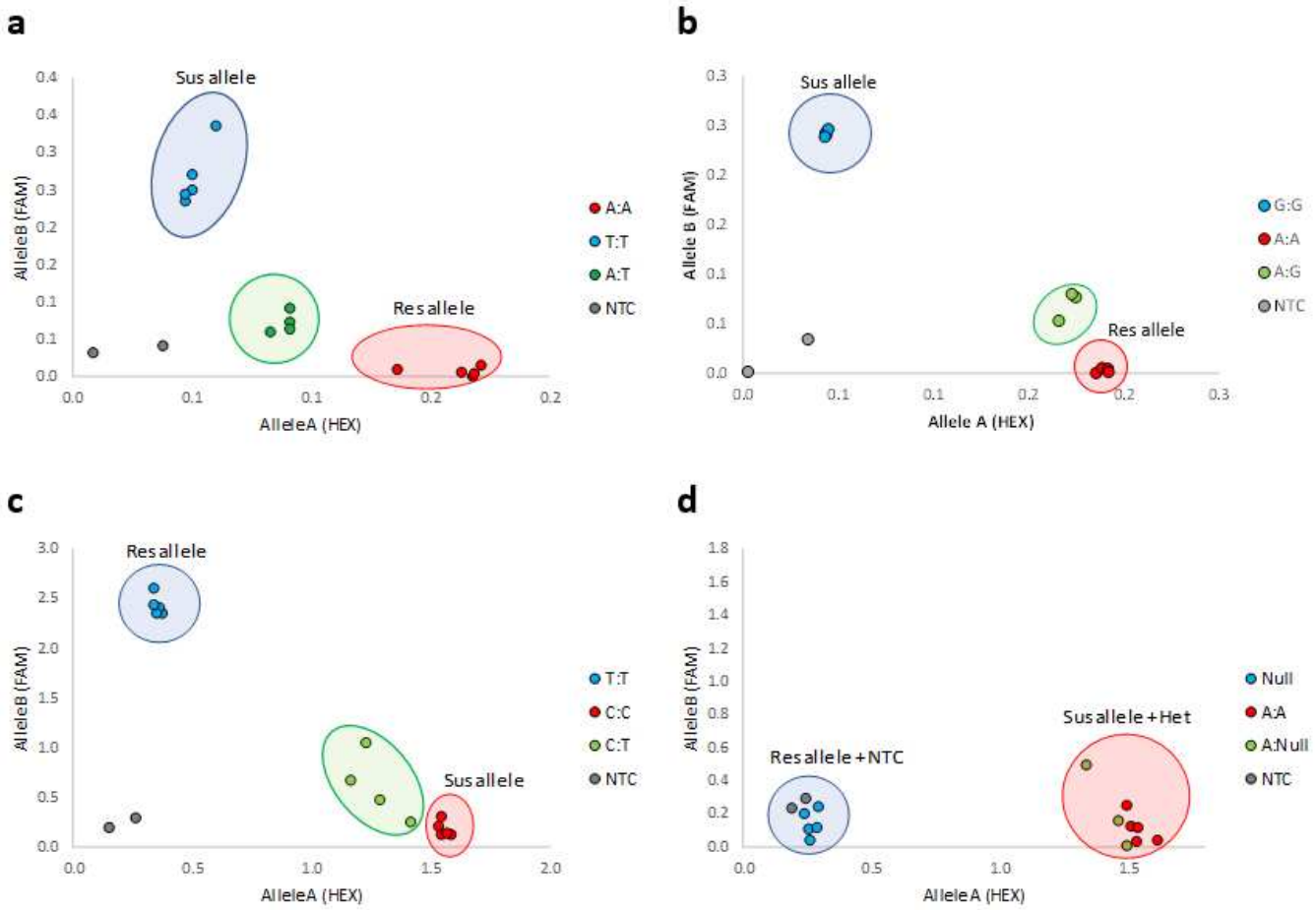

Figure 7

Examples of genotyping results for some of the KASP markers developed for the four most significant yellow rust resistance QTL (see Supplementary Table 2 for full details). Genotype calls for resistant (Res) and susceptible (Sus) alleles are indicated, derived from genomic DNA template from the founders subsequently indicated here. NTC = no template negative control. (A) QYr.niab-1A.1: KASP marker tplb0021i12_383 (DNA: Alchemy, susceptible allele; Hereward, resistant allele). (B) QYr.niab-2A.1: KASP marker BS00062679_51 (DNA: Xi19, resistant allele; Claire, susceptible allele). (C) QYr.niab-2B.1: KASP marker BS00016650_51 (DNA: Soissons, resistant allele; Robigus, susceptible allele). (D) QYr.niab-2D.1: KASP marker Kukri_c498_2381 (DNA: Claire, resistant allele; Soissons, susceptible allele).

Supplementary Files

This is a list of supplementary files associated with this preprint. Click to download.

- SupplementaryTable1.docx
- SupplementaryTable2.xlsx
- SupplementaryTable3.docx
- SupplementaryTable4.xlsx

- SupplementaryTable5.docx
- SupplementaryTable6.docx
- SupplementaryTable7.docx
- SupplementaryTable8.xlsx
- SupplementaryTable9.docx
- SupplementaryText.docx